DEI
DIPARTIMENTO DI
INGEGNERIA DELL'INFORMAZIONE

Università degli Studi di Padova

Dipartimento di Ingegneria dell' Informazione
Corso di Laurea Magistrale in Ingegneria dell' Automazione

Tesi di Laurea Magistrale

Multi-agent control strategies for optimal power flow in smart microgrids

Laureando
Marco Ruzza
Matricola 1034546

Relatore
Prof. Ruggero Carli

Correlatore
Dr. Guido Cavraro

Anno Accademico 2013-2014

Abstract

We consider the problem of minimizing the line power losses in a smart micro-grid by properly commanding the active and reactive power injections of the generators and supplying the required power demand to the loads. The minimization takes place with various constraints, that refer to the physical limits of the generators of providing a certain power injection.

We propose various strategies, based on gradient projection, dual-ascent and alternating direction multiplier method (ADMM), and with different assumptions on the capability of the nodes to compute, sense and communicate, but all having the common feature of being distributed and scalable. This kind of approach has been considered the most realistic and reasonable one, given the continuous growth (in width and complexity) of the electric grid.

A brief but useful theoretical dissertation is offered at the beginning, with the goal of providing a formal and accurate formulation of the problem. This part of the thesis recalls some basics about the AC circuits and the optimization problems, with particular attention on the convex ones and on the Lagrangian dualism.

Finally, simulations based on international test feeders are provided, in order to illustrate the behaviour and a sort of comparison of the algorithms.

Sommario

In questa tesi si affronta il problema di minimizzare la dissipazione di potenza lungo le linee in una smart micro-grid attraverso l'opportuna iniezione di potenza attiva e reattiva da parte dei generatori e provvedendo ai carichi la potenza richiesta. La minimizzazione avviene con alcuni vincoli, che si riferiscono ai limiti fisici dei generatori nel produrre un certo livello di potenza.

Vengono proposte diverse strategie, che si basano su metodi di tipo gradient projection, dual-ascent e sull'alternating direction multiplier method (ADMM), e con differenti assunzioni sulle capacità dei nodi di calcolare, misurare e comunicare, ma tutte con la caratteristica comune di essere distribuite e scalabili. Questo approccio è stato ritenuto il più realistico e ragionevole, data la continua crescita (in estensione e complessità) della rete elettrica.

All'inizio viene offerta una breve ma utile dissertazione teorica, allo scopo di fornire una formulazione formale ed accurata del problema. Questa parte della tesi presenta alcuni richiami riguardanti i circuiti a corrente alternata e i problemi di ottimizzazione, con particolare attenzione ai problemi convessi e al dualismo lagrangiano.

Infine vengono presentate alcune simulazioni basate su modelli di rete internazionali, al fine di illustrare il comportamento e il confronto degli algoritmi.

Contents

1 Introduction

1.1 Towards a new electric grid

In recent years the electric power distribution systems have been undergoing a deep renovation process in structure and functionality; these transformations refer to the introduction of advanced communication and control systems and of Distributed Energy Resources (DERs), that include renewable-based variable generation resources, e.g. photovoltaics or micro wind turbines, and new storage-capable loads, e.g. plug-in hybrid electric vehicles.

The causes behind this process are different: a great development of electronics and Information and Communication Technology (ICT), that allow to improve the efficiency of the energy distribution system; the increasing demand of electric energy, the need of guaranteeing the security and quality of supply but, on the contrary, the fast depletion of hydrocarbon reserves; the awareness of the institutions about the importance to have a sustainable environmental impact and, on the same principle, the birth of a new generation of low-impact vehicles.

In order to support this change, some international initiatives have arisen, like the US DOE *Smart Grids*[1] and the European counterpart *Smart Grids European Technology Platform*[2]. For the period 2003-2030, it has been estimated that in Europe alone about €500 billion of investment will be needed to upgrade the electricity transmission and distribution infrastructure [1].

In practice, it is happening an evolution from the traditional grid, characterized by:

- limited cross-border interconnections,
- centralised control,

[1] `http://energy.gov/oe/technology-development/smart-grid`
[2] `http://www.smartgrids.eu/`

- technology approaching an age of one century,
- large generating stations,
- optimisation for regional power adequacy,

to a new grid that allows to have :

- user specified quality, security and reliability of supply,
- flexible and optimal grid expansion, maintenance and operation,
- coordinated, local energy management and full integration of Distributed Generation (DG) and Renewable Energy Sources (RES) with large-scale central power generation,
- extensive small, distributed generation connected close to end customers [1].

In this scenario, the electricity distribution network is no longer an unidirectional channel that distributes energy from the big power plants to the small end-users, but becomes a *Smart Grid*, which is able to accept bidirectional flows, to make producers and consumers interact, to determine in advance the demand and, as a consequence, to provide the necessary flexibility for the production and consumption of electric energy. With the spread of distributed generation from renewable sources, also domestic, the integration of intelligent control modules with the already present components is required. Therefore, it is necessary to control and manage the production and distribution of electric power both in high and low voltage [2]. Figure 1.1 summarizes these concepts; it also shows how the control of distributed generators could be aggregated to form microgrids or "virtual" power plants to facilitate their integration.

A microgrid is a portion of low-voltage network which can be considered autonomous from the rest of the distribution system: in this way it is possible to achieve better quality of the service, higher efficiency and lower costs. Connected to the microgrid there are DERs, that can be divided into two categories: the loads (residential or industrial users), that may require a sinusoidal current which is not in phase with the voltage, and the microgeneration devices, that have not only to inject power into the microgrid (giving birth to the inverse flow mentioned before), but also to compensate reactive power, harmonic and voltage (also called *ancillary services*) [3]. These tasks can be achieved thanks to the power electronic interfaces (inverters) that represent the point of connection between every DER and the grid: in fact, even if the primary function of these interfaces is to control active power injection, when properly controlled they can also compensate the reactive power which in turn can be used for voltage control [6].

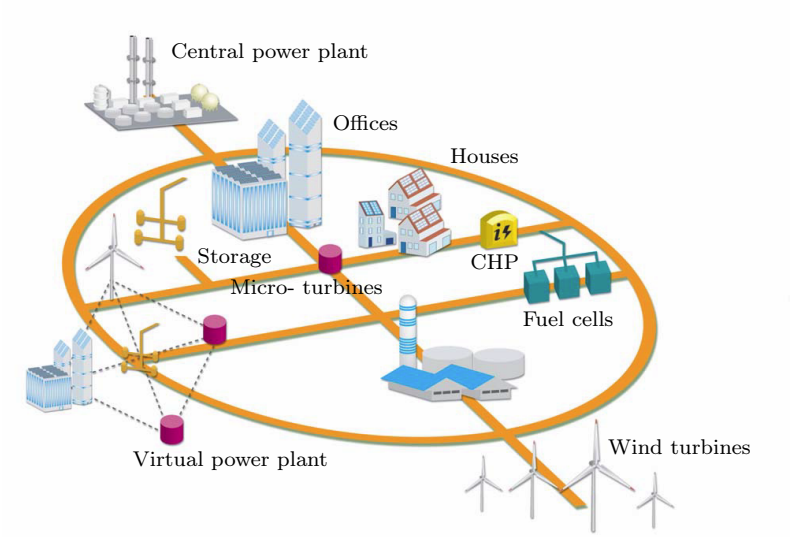

Figure 1.1: In the future, operation of system will be shared between central and distributed generators.

1.2 Multi-agent control approaches

In literature, many works have treated the problem of optimal active and reactive power generation for power losses minimization. However, most of them consider a central processing unit, that knows all the parameters of the grid and can access the whole grid state, sending to the generators (that are, usually, in small number) the power injection commands.

In this thesis we study the same problem, but in the context of networked control systems and distributed optimization. This kind of approach ensures scalability and adaptation in a dynamical context in which units can be likely inserted and removed. In this sense, as we will see, it is sufficient that every agent has a local knowledge of the grid parameters and topology, requiring an automatic reconfiguration of the grid control infrastructure (the *plug and play* approach) [11] when they are expected to connect and disconnect and a communication channel that allows to find out and to communicate with the other neighbouring agents (via, for example, *power line communication - PLC* - technology). It appeared to be the most reasonable choice given the size of the electric grid (and the inevitable growth) described so far.

Concretely, we propose some methods to solve the *optimal power flow* (*OPF*) problem in distribution networks that relies on the utilization of active and reactive power capable generators for a given pattern of power demand by the loads. The optimization will be done by imposing some physical constraints (upper and lower bounds) on the generation capabilities. In some cases, for a more accurate but also for a broader view of the problem, the deci-

sion variables are constituted by the bus voltages; however, the actual control mechanism to fix them are the active and reactive power injections on each node, allowing an easy comparison with those case in which the independent variables are precisely the power injections.

1.3 Short summary

The thesis consists of the following parts:

- Chapter 2, in which some basics on AC circuits are recalled, with particular attention on the phasorial notation and the electric power;
- Chapter 3, that explains the micro-grid model, the notation utilized in the work and the fundamental electric laws of the grid;
- Chapter 4, where the optimal power flow problem is formally stated and a brief background on optimization problems is given, with particular attention on the convex ones;
- Chapter 5, proposing an approach based on a gradient projection (or projected gradient) algorithm;
- Chapter 6, in which two different solutions based on a modified dual ascent algorithm are presented. The difference consists in the set of nodes which are actually able to measure and communicate (only the generators in the first case, all the nodes in the second one);
- Chapter 7, that shows an approach based on the Alternating Direction Multiplier Method (ADMM);
- Chapter 8, in which are proposed the plots of some meaningful simulations, with a brief but clear discussion on each one;
- in the end, Chapter 9 summarizes the most important aspects of the approaches, outlining possible future developments.

1.4 Notation

Here we introduce the operators we will use in the following. We do not list the whole set of symbols, that will be precisely defined in the text as soon as they appear for the first time.

$\lvert\cdot\rvert$	Both the absolute value of a quantity or the cardinality of a set, depending on the context.
$\lVert\cdot\rVert$	Euclidean norm for a vector or induced norm for a matrix, which is equal to the largest singular value if the matrix is a square matrix.
$\cdot^\top$	Transpose of a vector or matrix.
$\mathrm{Re}\{\cdot\}$	Real part of a complex quantity.
$\mathrm{Im}\{\cdot\}$	Imaginary part of a complex quantity.
$\bar{\cdot}$	Complex conjugate of a complex number or vector [3].
$\bar{\cdot}$, $\underline{\cdot}$	Upper and lower bound of a certain real quantity, respectively; used also for vectors with component-wise meaning [4].
$\otimes$	Kronecker product.
$[\cdot]_{ij}$	For a matrix, it refers to the component located in the i-th row and j-th column.
I_n	Identity matrix $\in \mathbb{R}^{n\times n}$.
$\mathbf{1}$	Vector whose components are all equal to one.
$\mathbf{1}_i$	Vector whose i-th component is equal to one, being all the others equal to zero.

[3] Both conjugate and transpose will be denoted as $\bar{\cdot}^\top$.

[4] Not to be confused with the complex conjugate operator, whose symbol is similar but not the same one. The context will help to distinguish between them.

2

Basics of AC circuits

In this chapter we recall some basics of electrical circuits regarding the alternating current that will be used in the following. Most of the concepts here introduced can be found, with some variations, in [7].

2.1 Phasorial representation

Let us consider a sinusoidal waveform described by:

$$a(t) = A_M \sin(\omega t + \alpha) \quad , \quad \omega = 2\pi f \tag{2.1}$$

where A_M is the amplitude, with the same physical dimension of $a(t)$, ω is the angular frequency expressed in [rad/s], being f the temporal frequency (with dimension [Hz]), and α is the (initial) phase, expressed in [rad].

If we consider the set of sinusoids with the same frequency, the signal described in Equation (2.1) is determined by the parameters A_M and α. These two parameters define one and only one complex number with modulus equal to $A_M/\sqrt{2}$ and argument equal to α:

$$A = \frac{A_M}{\sqrt{2}} e^{j\alpha} \tag{2.2}$$

which is called *phasor*.

Vice versa, from (2.2) it is possible to obtain one and only one waveform belonging to the set of waveforms with the same angular frequency ω, that is (2.1).

For periodic signals it is useful to introduce the *root mean square value*, defined by:

$$A_{\text{rms}} := \sqrt{\frac{1}{T} \int_T a(t)^2 dt} \tag{2.3}$$

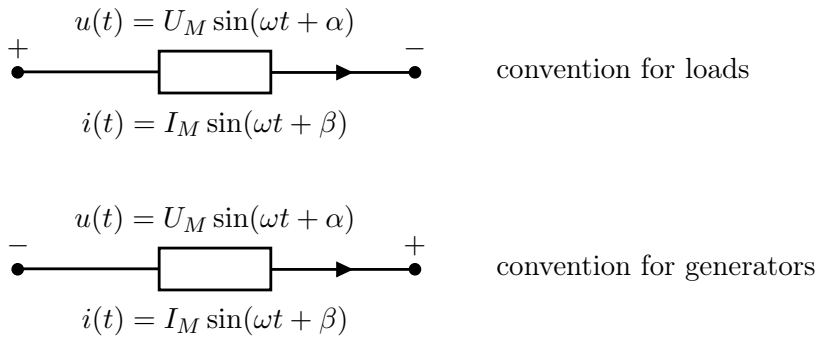

Figure 2.1

where $T = 1/f$ is the period of the signal; in the case of sinusoids we obtain:

$$A_{\text{rms}} = \frac{A_M}{\sqrt{2}} \tag{2.4}$$

Notice that equation (2.2) defines phasors by using the root mean square value transformation.

2.2 AC power

By considering the convention for loads (resp. generators) showed in Figure 2.1, we have that the *instantaneous power* absorbed (resp. generated) by the load (resp. generator) is:

$$\begin{aligned} p(t) &= u(t)i(t) = U_M \sin(\omega t + \alpha) I_M \sin(\omega t + \beta) \\ &= \frac{U_M I_M}{2} \cos(\alpha - \beta) - \frac{U_M I_M}{2} \cos(2\omega t + \alpha + \beta) \\ &= U_{\text{rms}} I_{\text{rms}} \cos\varphi - U_{\text{rms}} I_{\text{rms}} \cos(2\omega t + \alpha + \beta) \end{aligned} \tag{2.5}$$

where $\varphi := \alpha - \beta$.

The mean value in a period of the instantaneous power is called *active power* P:

$$P := \frac{1}{T} \int_T p(t)dt \overset{(2.5)}{=} U_{\text{rms}} I_{\text{rms}} \cos\varphi \tag{2.6}$$

the physical dimension of which is watt [W].

As a counterpart, the *reactive power* Q is defined:

$$Q := U_{\text{rms}} I_{\text{rms}} \sin\varphi \tag{2.7}$$

having dimension volt-ampere reactive [VAR].

The natural next step is the definition of the *apparent power* $|S|$:

$$|S| = U_{\text{rms}} I_{\text{rms}} \tag{2.8}$$

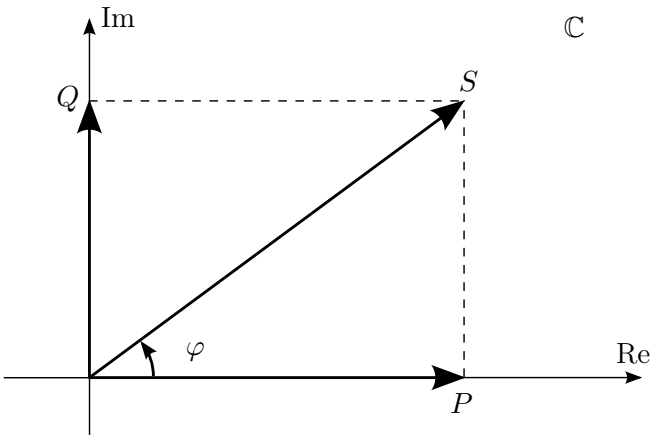

Figure 2.2

whose physical dimension is volt-ampere [VA]; at this point an useful factor can be introduced, referred to as *power factor* and defined by the ratio $P/|S|$, that is $\cos\varphi$.

From these definitions it is clear that the following equations hold:

$$|S| = \sqrt{P^2 + Q^2} \tag{2.9}$$

$$P = |S|\cos\varphi \quad , \quad Q = |S|\sin\varphi \tag{2.10}$$

In the end, it is possible to define the *complex power* S as the product of U and the complex conjugate $\bar{I}$ of I:

$$\begin{aligned} S := U\bar{I} &= U_{\text{rms}}e^{j\alpha}I_{\text{rms}}e^{j(-\beta)} = U_{\text{rms}}I_{\text{rms}}e^{j(\alpha-\beta)} \\ &= |S|e^{j\varphi} = |S|(\cos\varphi + j\sin\varphi) = P + jQ \end{aligned} \tag{2.11}$$

expressed again in [VA] and that allows to underline the equations:

$$\varphi = \angle S \quad , \quad P = \text{Re}\{S\} \quad , \quad Q = \text{Im}\{S\} \tag{2.12}$$

evidently being the apparent power $|S|$ the modulus of the complex power S. Figure 2.2 shows the relations between these physical quantities on the complex plane.

It is important to underline that a passive element (load) with the convention for loads must have $P \geq 0 \Leftrightarrow \cos\varphi \geq 0 \Leftrightarrow -\frac{\pi}{2} \leq \varphi \leq \frac{\pi}{2}$.

2.3 Impedance and admittance

Once we defined the phasors for sinusoidal waveforms, we define the *impedance* Z of a passive element[1] as:

$$Z := \frac{U}{I} \tag{2.13}$$

[1] for active elements (generators), the phasors of voltage and current are not a priori correlated.

expressed in ohm [Ω]; written in both polar and Cartesian forms gives:

$$\begin{aligned} Z = \frac{U_{\text{rms}}}{I_{\text{rms}}} e^{j(\alpha-\beta)} = \frac{U_{\text{rms}}}{I_{\text{rms}}} e^{j\varphi} \;\Rightarrow\; \begin{cases} |Z| = \dfrac{U_{\text{rms}}}{I_{\text{rms}}} = \dfrac{U_M}{I_M} \quad [\Omega] \\ \angle Z = \varphi \quad [\text{rad}] \end{cases} \\ = |Z| e^{j\varphi} \;\Rightarrow\; \begin{cases} R := \text{Re}\{Z\} = |Z| \cos\varphi \quad \textit{resistance } [\Omega] \\ X := \text{Im}\{Z\} = |Z| \sin\varphi \quad \textit{reactance } [\Omega] \end{cases} \end{aligned} \tag{2.14}$$

Observe that the condition $\cos\varphi \geq 0$ implies $\text{Re}\{Z\} \geq 0$. At this point, the power absorbed by the passive element is:

$$S = U\bar{I} = ZI\bar{I} = ZI^2 \rightarrow \begin{cases} S = ZI^2 \\ P = RI^2 \\ Q = XI^2 \end{cases} \tag{2.15}$$

Related to the impedance, we also define the *admittance* Y as:

$$Y := \frac{1}{Z} = \frac{I}{U} \tag{2.16}$$

expressed in siemens [S]; written in both polar and Cartesian forms gives:

$$\begin{aligned} Y = \frac{I_{\text{rms}}}{U_{\text{rms}}} e^{j(\beta-\alpha)} = \frac{I_{\text{rms}}}{U_{\text{rms}}} e^{-j\varphi} \;\Rightarrow\; \begin{cases} |Y| = \dfrac{I_{\text{rms}}}{U_{\text{rms}}} = \dfrac{I_M}{U_M} \quad [\text{S}] \\ \angle Y = -\varphi \quad [\text{rad}] \end{cases} \\ = |Y| e^{-j\varphi} \;\Rightarrow\; \begin{cases} G := \text{Re}\{Y\} = |Y| \cos\varphi \quad \textit{conductance } [\text{S}] \\ B := \text{Im}\{Y\} = -|Y| \sin\varphi \quad \textit{susceptance } [\text{S}] \end{cases} \end{aligned} \tag{2.17}$$

Again, the power entering in the passive element can be written as:

$$S = U\bar{I} = U\bar{Y}\bar{U} = \bar{Y}U^2 \rightarrow \begin{cases} S = YU^2 \\ P = GU^2 \\ Q = -BU^2 \end{cases} \tag{2.18}$$

By using the physical quantities introduced above and the equations describing the behaviour, respectively, of resistors, inductors and capacitors (2.19):

$$u(t) = Ri(t)\ ,\ v(t) = L\frac{d}{dt}i(t)\ ,\ i(t) = C\frac{d}{dt}v(t) \tag{2.19}$$

we obtain the expressions written in Table 2.1.

2.4 Analysis of AC circuits

Thanks to phasors, the techniques for solving Direct Current circuits can be applied to solve AC circuits. The procedure to follow is:

Table 2.1: Important values for resistors, inductors and capacitors.

physical quantity	resistor R	inductor L	capacitor C
φ	0	$\frac{\pi}{2}$	$-\frac{\pi}{2}$
impedance Z	R	$j\omega L$	$j\frac{-1}{\omega C}$
admittance Y	G	$j\frac{-1}{\omega L}$	$j\omega C$
complex power S	$RI^2 = GU^2$	$j\omega LI^2 = j\frac{1}{\omega L}U^2$	$j\frac{-1}{\omega C}I^2 = j(-\omega CU^2)$

1. to turn the known sinusoidal quantities in phasors,
2. to apply the principles and theorems for DC circuits to phasors,
3. to return to the time domain by calculating the sinusoidal signals starting from the obtained phasors.

In this sense, apart of the generalized Ohm's we have used for the definition of impedance, we recall at least Kirchhoff's current law (KCL) - the algebraic sum of currents in a network of conductors meeting at a point is zero:

$$\sum \pm I = 0 \qquad \text{(KCL)} \tag{2.20}$$

and Kirchhoff's voltage law (KVL) - the voltage drop around any closed loop is equal to zero:

$$\sum \pm U = 0 \qquad \text{(KVL)} \tag{2.21}$$

In the following, we will consider the electrical quantities only as phasors, being the time-domain expressions quickly obtainable.

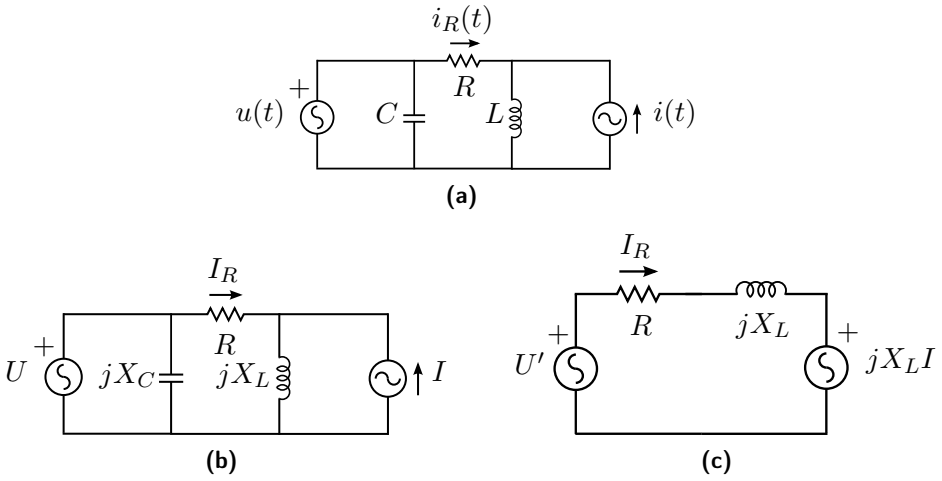

Figure 2.3: Circuits for Example 2.1.

EXAMPLE 2.1

Consider the electrical circuit shown in Figure 2.3a. Given the quantities $u(t) = \sqrt{3} \cdot 150 \cos(\omega t - \pi/4)$ V, $i(t) = 10 \sin(\omega t - 3\pi/4)$ A, $R = 15\ \Omega$, $X_L = \sqrt{3} \cdot 15\ \Omega$ and $X_C = -10\ \Omega$, calculate $i_R(t)$.

The first step is to find the phasors of $u(t)$ and $i(t)$. Observing that $u(t) = \sqrt{3} \cdot 150 \cos(\omega t - \pi/4) = \sqrt{3} \cdot 150 \sin(\omega t + \pi/4)$, we obtain:

$$U = \frac{\sqrt{3}}{\sqrt{2}} \cdot 150[\cos(\pi/4) + j \sin(\pi/4)] = \sqrt{3} \cdot 75(1 + j)$$

$$I = \frac{10}{\sqrt{2}}[\cos(-3\pi/4) + j \sin(-3\pi/4)] = 5(-1 - j)$$

that give Figure 2.3b. We can now reduce the circuit to the one shown in Figure 2.3c by using the equations:

$$U' = U \quad , \quad I_R = \frac{U' - jX_LI}{R + jX_L}$$

obtaining:

$$I_R = \sqrt{3} \cdot 2.5(\sqrt{3} + j)$$

In the end, we calculate $i_R(t)$ as:

$$i_R(t) = \sqrt{2}|I_R| \sin(\omega t + \angle I_R)$$

with

$$|I_R| = \sqrt{6} \cdot 2.5 \cdot \sqrt{3 + 1} = 5\sqrt{6} \quad , \quad \angle I_R = \arctan(1/\sqrt{3}) = \pi/6 \quad .$$

3 Grid modeling

In the first part of this chapter a model for the electric power system is presented: most of the electrical concepts here introduced can be found in [8], while the graph model is well described in [3]. The subsequent section is about the cyber layer, where communication and computation take place [11].

3.1 Physical layer

The physical layer is constituted by the power distribution infrastructure (that is, the grid itself), including transmission lines, microgenerators and loads. All the theory presented in Chapter 2 can be used if the system is in steady state operation, that happens when all voltages and currents are sinusoidal signals at the same frequency. It is obvious that this condition is not verified all the time: in a power system there are always switching actions, load changes and other operations that make most of the variables vary with the time. However, these variations are most of the time so small and fast that a time-invariant model of the power system is justified.

3.1.1 Graph structure

A microgrid can be modelled as a directed graph $\mathcal{G}$ in which edges (also called *branches*) represent the power lines, and nodes (also called *buses*) represent both loads and generators (including the point of connection of the microgrid to the transmission grid, called *PCC*, point of common coupling).

The graph is directed in order to distinguish, for every edge, the node which is nearer (from a topological point of view) to the PCC: this node is considered as the source node, being the other one the terminal node.

Let then $\mathcal{G} = (\mathcal{V}, \mathcal{E}, \sigma, \tau)$ be a directed graph, where:

- $\mathcal{V}$ is the set of nodes, with $|\mathcal{V}| =: n$; among these ones, we denote by $\mathcal{C} \subset \mathcal{V}$ the set of microgenerators, including the PCC, with $|\mathcal{C}| =: m$;
- $\mathcal{E}$ is the set of edges,
- σ and τ are two functions defined as

$$\sigma : \mathcal{E} \to \mathcal{V}$$
$$e \mapsto \sigma(e) \text{ , the source node}$$

and

$$\tau : \mathcal{E} \to \mathcal{V}$$
$$e \mapsto \tau(e) \text{ , the terminal node.}$$

The *path* $\mathcal{P}_{hk} = (v_1, \ldots, v_l)$ from a given node h to another given node k is the sequence of nodes, without repetitions, such that

- $v_1 = h$
- $v_l = k$
- $\forall i = 1, \ldots, l-1$, the nodes v_i and v_{i+1} are connected by an edge.

The interconnections between the different nodes can be represented by the *incidence matrix* $A \in \{0, \pm 1\}^{|\mathcal{E}| \times n}$, that has the elements in position (e, v) equal to

$$[A]_{ev} = \begin{cases} -1 & \text{if } v = \sigma(e) \\ 1 & \text{if } v = \tau(e) \\ 0 & \text{otherwise.} \end{cases}$$

3.1.2 Transmission lines

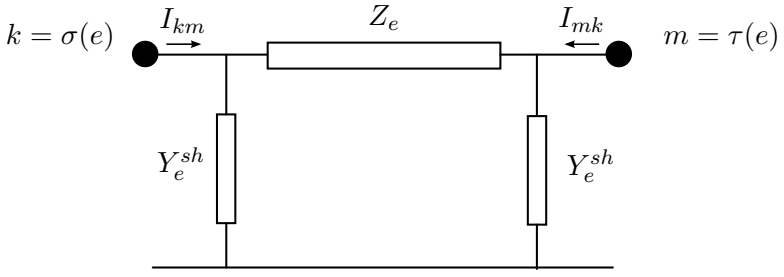

Figure 3.1: Lumped-circuit model (π-model) of a transmission line between nodes k and m.

For a transmission line e it is possible to derive a π-model (Figure 3.1) that is characterized by the parameters $Z_e = R_e + jX_e$, the series impedance

[Ω], and by $Y_e^{sh} = G_e^{sh} + jB_e^{sh}$, the shunt admittance [S]. The two shunt elements are assumed to be equal, which is true for homogeneous lines. For real transmission lines all the parameters R_e, X_e, G_e^{sh} and B_e^{sh} are positive, and usually G_e^{sh} is so small that could be neglected.

The following equations hold for complex currents and voltages:

$$I_{km} = \frac{U_k - U_m}{Z_e} + Y_e^{sh} U_k \quad , \quad I_{mk} = \frac{U_m - U_k}{Z_e} + Y_e^{sh} U_m \tag{3.1}$$

that can be written in matrix form as:

$$\begin{bmatrix} I_{km} \\ I_{mk} \end{bmatrix} = \begin{bmatrix} Y_e + Y_e^{sh} & -Y_e \\ -Y_e & Y_e + Y_e^{sh} \end{bmatrix} \begin{bmatrix} U_k \\ U_m \end{bmatrix} \tag{3.2}$$

with $Y_e := Z_e^{-1}$. The homogeneity of the cables is reflected on the 2×2 matrix of Equation (3.2), that is symmetric and with equal diagonal values.

For this work, we take these further

Assumptions

1. the shunt admittance Y_e^{sh} can be neglected; therefore, we consider only the line impedance Z_e that allows to write

$$I_e = I_{km} = -I_{mk} = \frac{U_{\sigma(e)} - U_{\tau(e)}}{Z_e}$$

2. all transmission lines in the microgrid have the same inductance/resistance ratio: it is then possible to write the diagonal matrix of line impedances $\boldsymbol{Z} = \mathrm{diag}(Z_1, \ldots, Z_m)$ as

$$\boldsymbol{Z} = e^{j\theta} Z$$

where Z is a diagonal real-valued matrix, whose elements are $[Z]_{ee} = |Z_e|$.

3.1.3 Loads and generators

Loads and generators are modelled respectively as negative and positive power injections to the bus k where they are connected (Figure 3.2).

We model the PCC (labeled as node 1) as a sinusoidal voltage generator with nominal voltage U_N and an arbitrary fixed angle φ:

$$U_{PCC} = U_N e^{j\varphi} \tag{3.3}$$

Loads and microgenerators (i.e. every node v except the PCC) are modelled through the following law relating the complex voltage U_v and the complex current I_v:

$$U_v \bar{I}_v = S_v \tag{3.4}$$

From the active power $P_v = \mathrm{Re}\{S_v\}$ it is possible to distinguish between loads, that are passive elements and have $P_v < 0$, and generators, that inject active power into the grid and characterized by $P_v \geq 0$.

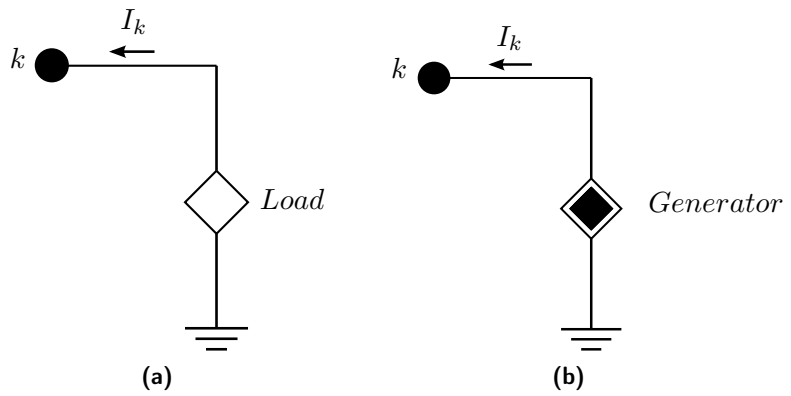

Figure 3.2: Symbols for loads and generators.

3.1.4 Transformers

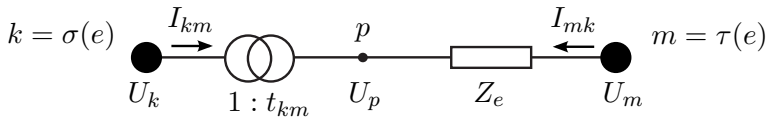

Figure 3.3: Transformer model with complex ratio $t_{km} = a_{km}e^{j\psi}$.

The model of a transformer is constituted by an ideal transformer with turns ratio

$$t_{km} := U_p/U_k = a_{km}e^{j\psi} \tag{3.5}$$

in series with an impedance Z_e, as shown in Figure 3.3. Depending on if t_{km} is real ($\psi = 0$) or complex ($\psi \neq 0$), the transformer is in-phase or phase-shifting.

Because there are not power losses (neither active nor reactive) in the ideal transformer, we have that:

$$U_k\bar{I}_{km} + U_p\bar{I}_{mk} = 0 \tag{3.6}$$

It is now simple to verify that the following equation holds:

$$\begin{bmatrix} I_{km} \\ I_{mk} \end{bmatrix} = \begin{bmatrix} a_{km}^2 Y_e & -\bar{t}_{km}Y_e \\ -t_{km}Y_e & Y_e \end{bmatrix} \begin{bmatrix} U_k \\ U_m \end{bmatrix} \tag{3.7}$$

Notice that this matrix is not symmetric if t_{km} is not real, and the diagonal elements are not equal if $a_{km}^2 \neq 1$.

Transformers have been described only for completeness of explanation: in fact, dealing with a low voltage power distribution network, transformers are neglected (the only one is physically constituted by the PCC).

3.1.5 Grid equations

The steady state of the microgrid is described by the system variables:

- $u \in \mathbb{C}^n$, where $u_i = |U_i|e^{j\angle U_i}$ is the complex grid voltage at node i;
- $i \in \mathbb{C}^n$, where $i_i = |I_i|e^{j\angle I_i}$ is the complex current injected by node i;
- $\xi \in \mathbb{C}^{|\mathcal{E}|}$, where $\xi_e = |\xi_e|e^{j\angle \xi_e}$ is the complex current flowing on edge e.

Kirchhoff's current law at the nodes and the voltage drop on the edges of the graph are described, respectively, by the equations:

$$A^\top \xi + i = 0 \tag{3.8}$$

$$Au + e^{j\theta} Z\xi = 0 \tag{3.9}$$

From (3.8) and (3.9) it is easy to obtain

$$i = e^{-j\theta} A^\top Z^{-1} Au = e^{-j\theta} Yu \tag{3.10}$$

where $Y := A^\top Z^{-1} A$ is the *weighted Laplacian* of the graph and $\boldsymbol{Y} = e^{-j\theta} Y$ represents the *nodal admittance* matrix in power system analysis.

3.2 Cyber layer

The cyber layer constitutes the intelligent part of the smart grid: it is the set of all the sensors, actuators, communication systems and devices with computational capabilities.

All the intelligent devices just described can be referred to as *agents*, the set $\mathcal{A}$. Depending on the configuration, in this work the agents will be constituted in turn by only the generators or by all the nodes. Each agent is able to measure the voltage (both amplitude and angle, through for example a phasor measurement unit, PMU) of the node it corresponds to, to command the amount of the reactive power injection of it, and to communicate with other agents via some communication channel (for example, via power line communication, PLC [11]).

It is now useful to introduce the following

Definition 1 (*Neighbours in the cyber layer*)**.** Consider an agent of the cyber layer $h \in \mathcal{A}$. The set of neighbours of h in the cyber layer, denoted as $\mathcal{N}(h)$, is the subset of $\mathcal{A}$ defined as

$$\mathcal{N}(h) = \{k \in \mathcal{A} \mid \forall \mathcal{P}_{hk}, \mathcal{P}_{hk} \cap \mathcal{A} = \{h, k\}\} \ .$$

It is assumed that every agent knows its set of neighbours and can communicate with them.

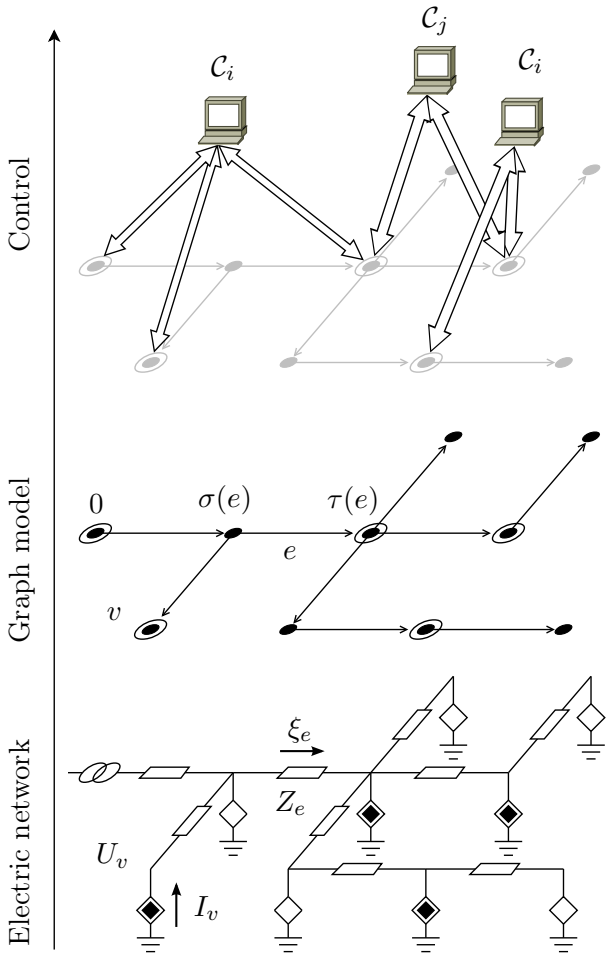

Figure 3.4: Representation of the cyber-physical model of the grid. In this case, only the generators are assumed to be smart agents.

4 Problem formulation

In this chapter the Optimal Power Flow (OPF) problem is described, with a detailed discussion about its most important characteristics. It is then exploited as a start point for a more generalized dissertation on the optimization problems.

4.1 Optimal Power Flow Problem

In general, the Power Flow (PF) problem consists in calculating the set of voltages and flows in a network corresponding to a given pattern of load and generation. These quantities are found by solving a set of equations of the form:

$$h_i(x) = 0 \quad i = 1, \dots, p \tag{4.1}$$

obtained by expressing the nodal power balance equations. The Optimal Power Flow (OPF) problem, instead, generally consists in solving a constrained optimization problem of the form:

$$\begin{aligned} \underset{x}{\text{minimize}} \quad & f(x) && \text{(4.2a)} \\ \text{subject to} \quad & g_i(x) \leq 0 \quad i = 1, \dots, m && \text{(4.2b)} \\ & h_j(x) = 0 \quad j = 1, \dots, p && \text{(4.2c)} \end{aligned}$$

where $f(x)$ is the cost function that has to be minimized, which is dependent on some quantities x of the grid, inequalities $g_i(x)$ give some necessary (or for proper functioning) physical bounds to the electrical quantities of the grid and (4.2c) represent, as before, the nodal power equations.

In this thesis, the objective is to minimize the power distribution losses:

$$J_{\text{losses}} := \sum_{e \in \mathcal{E}} |\xi_e|^2 \operatorname{Re}(z_e)$$

given suitable lower and upper bounds on the values of active and reactive power of every node; our problem can then be expressed as:

$$\begin{aligned} &\text{minimize} && J_{\text{losses}} && && (4.3a)\\ &\text{subject to} && \underline{p}_i \le p_i \le \bar{p}_i && && (4.3b)\\ &&& \underline{q}_i \le q_i \le \bar{q}_i && i \in \mathcal{V} && (4.3c) \end{aligned}$$

and subject to the physical laws of the grid. The inequalities (4.3b) and (4.3c) refers to the physical limitation on the generation capability of node i if it is a generator, with $\underline{p}_i = \overline{p}_i$ and $\underline{q}_i = \overline{q}_i$ fixed if i is a load.

The goal is to represent the problem by using only one physical quantity of the grid, imposing the satisfaction of the electric laws by expressing some of them as function of the independent ones: in this way, the equality constraints (4.2c) can be included in the cost function, letting only the inequality constraints. We discuss two different approaches, that are related to the control strategies we are going to use:

1. active and reactive power vectors p and q are used as the decisional variables. This approach will be used in the gradient projection and dual ascent control strategies. While the inequality constraints are trivial, for the cost function an approximation will be used, whose accuracy is guaranteed by the typical high value of the nominal voltage and by the feedback law itself.

2. node voltages u are considered as the independent variables: they well describe the state of the grid and allow to have an expression of the problem with fewer approximations - an essential feature for an open loop control strategy as the one based on the ADMM we will treat in the following.

4.2 Optimization problems

In order to classify and solve the OPF problem proposed, we introduce some basics about the optimization problems, with a particular attention to the convex ones. Most of concepts here considered are taken from [15].

4.2.1 Optimal and locally optimal points

Consider the optimization problem in standard form (4.2). Apart from the OPF problem there introduced, in general $x \in \mathbb{R}^n$ is the *optimization variable*, $f : \mathbb{R}^n \to \mathbb{R}$ is the *objective* or *cost function*, $g_i : \mathbb{R}^n \to \mathbb{R}$, $i = 1, \dots, m$ are the *inequality constraint functions* and $h_i : \mathbb{R}^n \to \mathbb{R}$, $i = 1, \dots, p$ are the *equality*

constraint functions. The *optimal value* p^* is defined as

$$p^* = \inf\{f(x) |\ g_i(x) \leq 0,\ i = 1, \ldots, m,\ h_j(x) = 0,\ j = 1, \ldots, p\}$$

If the problem is unbounded below it is clear that $p^* = -\infty$; more interesting is when the problem is *infeasible*, i.e. no x satisfies the constraints, in which case it is considered $p^* = \infty$. As we can imagine, x is *feasible* if $x \in \mathrm{dom} f$ and satisfies the constraints, x is *optimal* if it is feasible and $f(x) = p^*$, while x is *locally optimal* if there exists an $R > 0$ such that x is optimal for

$$\begin{array}{ll} \underset{z}{\text{minimize}} & f(z) \\ \text{subject to} & g_i(z) \leq 0 \quad i = 1, \ldots, m \\ & h_j(z) = 0 \quad j = 1, \ldots, p \\ & \|z - x\| \leq R \end{array}$$

All the functions of the optimization problem determine the *domain* of the problem, that can be considered an implicit constraint in addition to explicit ones seen so far:

$$\mathcal{D} = \mathrm{dom}\, f \cap \bigcap_{i=1}^{m} \mathrm{dom}\, g_i \cap \bigcap_{i=1}^{p} \mathrm{dom}\, h_i \tag{4.4}$$

As we said, an important class is represented by the convex optimization problems, where convexity, of course, has a central role.

A *set* $\mathcal{C}$ is *convex* if it contains the line segment between any two points in the set:

$$x_1, x_2 \in \mathcal{C},\ 0 \leq \theta \leq 1 \ \Rightarrow\ \theta x_1 + (1 - \theta) x_2 \in \mathcal{C}$$

A *function* $f : \mathbb{R}^n \to \mathbb{R}$ is *convex* if $\mathrm{dom}\, f$ is a convex set and

$$f(\theta x + (1 - \theta) y)) \leq \theta f(x) + (1 - \theta) f(y) \quad \forall x, y \in \mathrm{dom}\, f,\ 0 \leq \theta \leq 1$$

An *optimization problem* is *convex* if the cost function f and the inequalities constraint functions g_i are convex and the equality constraints h_i are linear.

The linearity of the equality constraints can be visualized by writing the problem in the *standard form of convex optimization problem*

$$\begin{array}{ll} \underset{x}{\text{minimize}} & f(z) \\ \text{subject to} & g_i(x) \leq 0 \quad i = 1, \ldots, m \\ & a_i^\top x = b_i \quad j = 1, \ldots, p \end{array}$$

The two most important properties of the convex optimization problems are formulated in the following theorems.

Proposition 1. *The set of feasible points of a convex problem is convex.*

Proof. Being the intersection of convex sets still convex, the domain $\mathcal{D}$ as expressed in (4.4) is a convex set. At this point, the set of feasible points of a convex problem is the intersection of its domain $\mathcal{D}$, which is convex, and m convex sets of the form $\{x|g_i(x) \leq 0\}$ and p hyperplanes $\{x|a_i^\top x = b_i\}$, then it is convex. □

Theorem 1. *Any locally optimal point of a convex problem is a globally optimal.*

Proof. Let x be a locally optimal point and y an optimal point with $f(x) > f(y)$. Then there exists an $R > 0$ such that, for any feasible z, the following implication holds:

$$\|z - x\| < R \Rightarrow f(z) \geq f(x)$$

Consider a z parametrized as $z = \theta y + (1 - \theta)x$ with $\theta = \dfrac{R}{2\|y - x\|}$. Because $\|y - x\| > R$, it must be $0 < \theta < 1/2$. We also have that z is feasible, since it is a convex combination of two feasible points, and its euclidean distance from x is equal to:

$$\|z - x\| = \|(1 - \theta)x + \theta y - x\| = \|\theta(y - x)\| = \frac{R}{2\|y - x\|}\|y - x\| = \frac{R}{2} < R$$

Then, since f is convex, we have

$$f(z) = f(\theta y + (1 - \theta)x) \leq \theta f(y) + (1 - \theta)f(x) < \theta f(x) + (1 - \theta)f(x) = f(x)$$

which contradicts our assumption that x is locally optimal. □

As we can argue, the OPF problem might not be convex in general: the relations between voltages and power injections of the nodes are non-linear.

Traditional techniques for general nonconvex problems involve compromises: some methods, based on the nonlinear programming, are fast and can handle large problems, but can only find local optimal points, which are dependent on the initial guess, and provide no information about distance to (global) optimum; on the contrary, the so-called global optimization methods find the global solution but worst-case complexity grows exponentially. What is most interesting is that these algorithms are often based on solving complex subproblems. In nonconvex problems, in fact, convex optimization has multiple roles:

- initialization for local optimization;
- convex heuristics for nonconvex optimization;

- bounds for local optimization; two common methods are:
  - relaxation: each non convex constraint is replaced with a looser, but convex, constraint;
  - Lagrangian relaxation: the Lagrangian dual problem is solved. It is convex and provides a lower bound.

4.2.2 Lagrange dual problem

The idea behind the Lagrangian dualism is to think about the constraints as part of the cost function: more precisely, we define the *Lagrangian* as

$$\mathcal{L}(x, \lambda, \mu) = f(x) + \sum_{i=1}^{m} \lambda_i g_i(x) + \sum_{i=1}^{p} \mu_i h_i(x) \tag{4.5}$$

which consists in a weighted sum of objective and constraint functions, with λ and μ which are referred to as the *Lagrange multipliers*.

The Lagrangian just defined allows to introduce the *Lagrange dual function*

$$d(\lambda, \mu) = \inf_{x \in \mathcal{D}} \mathcal{L}(x, \lambda, \mu) \tag{4.6}$$

The Lagrange dual function has the following properties that make it very useful:

- $\forall \lambda \geq 0$ and $\forall \mu$ we have $d(\lambda, \mu) \leq p^*$, and this fact can be used to find a more or less accurate lower bound for the optimal value p^* [1];
- it is concave, since it is the pointwise minimum of a family of linear functions of (λ, μ).

The consequence is that the *dual problem* defined as

$$\begin{aligned} &\text{maximize} && d(\lambda, \mu) \\ &\text{subject to} && \lambda \geq 0 \end{aligned}$$

aims to find the best lower bound d^* on p^* obtainable from Lagrange dual function and has the very important feature to be a convex optimization problem, because the function that has to be maximized is concave (it is equivalent to minimize $-d(\lambda, \mu)$, which is convex) and the inequality constraint is convex.

At this point, we are interested on the precision of d^* as lower bound. We have seen that in general $d^* \leq p^*$: this case always holds, both for convex and

[1] *Proof.* If $\tilde{x}$ is feasible and $\lambda \geq 0$, then (remembering that $g_i \leq 0$ and $h_i = 0$, $\forall i$)

$$f(\tilde{x}) \geq \mathcal{L}(\tilde{x}, \lambda, \mu) \geq \inf_{x \in \mathcal{D}} \mathcal{L}(x, \lambda, \mu) = d(\lambda, \mu) \qquad \square$$

nonconvex problems, and is denoted as *weak duality*. However, there are some cases in which we are able to find a "perfect" lower bound, with $d^* = p^*$: it is common to denote this situation as *strong duality*, or by saying that *zero duality gap* occurs.

By relying on the results presented in [14], which show that strong duality holds for OPF problems under some commonly verified practical conditions, we will provide a distributed algorithm for the OPF problem, which makes use of the Lagrangian relaxation and attempts to solve the (simpler, respect to the original one) Lagrange dual problem.

5

Gradient Projection approach

In this chapter we propose a solution for the optimal power flow (4.3) which is based on the Gradient Projection algorithm (see, for example, [17]).

As said in the previous chapter, the independent variables of the problem are chosen to be the active and reactive power injections of the generators, p_G and q_G, respectively. In order to include the relations between the electric quantities directly into the cost function, we first express the cost function in terms of another suitable physical quantity, the node voltages u, later providing an expression in terms of p_G and q_G. By using (3.8) and (3.9), the power losses can be expressed as function of the node voltages (see Appendix A), obtaining:

$$J_{\text{losses}} = \bar{u}^\top Y u \cos\theta \tag{5.1}$$

The expression of u in terms of p and q can be obtained thanks to the following lemma and proposition.

Lemma 1. *Let Y be the Laplacian $Y = A^\top Z^{-1} A$. There exists a unique symmetric positive definite matrix $X \in \mathbb{R}^{n\times n}$ such that*

$$\begin{cases} XY = I - \mathbf{1}\mathbf{1}_0^\top \\ X\mathbf{1}_0 = 0 \end{cases}$$

Proof. See Lemma 1 in [3]. □

The matrix X depends only on the topology of the grid and on the impedances of its power lines; by adopting the block decomposition

$$u = \begin{bmatrix} u_1 \\ u_G \\ u_L \end{bmatrix} \quad , \quad s = p + jq = \begin{bmatrix} p_1 + jq_1 \\ p_G + jq_G \\ p_L + jq_L \end{bmatrix}$$

where the subscript $_G$ denotes the set of all the *generators*, except the PCC, which is referred to as node 1, and $_L$ represents the set of the *loads*, we have

$$X = \begin{bmatrix} 0 & \mathbf{0} & \mathbf{0} \\ \mathbf{0} & M & N \\ \mathbf{0} & N^\top & O \end{bmatrix} \quad , \quad M \in \mathbb{R}^{(m-1)\times(m-1)}, \quad N \in \mathbb{R}^{(m-1)\times(n-m)}$$

The approximate relation between voltages and power injection is finally provided by the following

Proposition 2. *In the physical model described by (3.3), (3.4), (3.8) and (3.9), node voltages satisfy*

$$\begin{bmatrix} u_1 \\ u_G \\ u_L \end{bmatrix} = e^{j\varphi}\left(U_N \mathbf{1} + \frac{e^{j\theta}}{U_N} \begin{bmatrix} 0 & \mathbf{0} & \mathbf{0} \\ \mathbf{0} & M & N \\ \mathbf{0} & N^\top & O \end{bmatrix} \begin{bmatrix} 0 \\ \bar{s}_G \\ \bar{s}_L \end{bmatrix} \right) + o\left(\frac{1}{U_N}\right)$$

where the little-o notation means that $\lim_{U_N \to \infty} \frac{o(f(U_N))}{f(U_N)} = 0$

Proof. The proposition is a direct consequence of Proposition 1 in [3]. □

After some algebraic computations that can be found in A.1, we obtain

$$\begin{aligned} \bar{u}^\top Y u &\approx \frac{p^\top X p}{U_N^2} + \frac{q^\top X q}{U_N^2} \\ &= \frac{1}{U_N^2}\left(p_G^\top M p_G + 2 p_L^\top N^\top p_G + p_L^\top O p_L^\top + q_G^\top M q_G + 2 q_L^\top N^\top q_G + q_L^\top O q_L^\top\right) \end{aligned} \tag{5.2}$$

Therefore, besides some positive constants, our problem is equivalent to minimize the function

$$f = \frac{1}{2}\left(p_G^\top M p_G + 2 p_L^\top N^\top p_G + p_L^\top O p_L^\top + q_G^\top M q_G + 2 q_L^\top N^\top q_G + q_L^\top O q_L^\top\right)$$

At this point we have to calculate the gradient of this last expression with respect to the vector $\begin{bmatrix} p_G^\top & q_G^\top \end{bmatrix}^\top$, that represents the set of all the decisional variables. We obtain:

$$\nabla f = \begin{bmatrix} \dfrac{\partial f}{\partial p_G} \\ \dfrac{\partial f}{\partial q_G} \end{bmatrix} = \begin{bmatrix} M p_G + N p_L \\ M q_G + N q_L \end{bmatrix}$$

The problem of the obtained expression is due to the dependence on p_L and q_L, which are assumed to be unknown. However, thanks to Proposition 2 they can be easily expressed as functions of u_G, that are monitored. We have:

$$u_G = e^{j\varphi}\left(U_N \mathbf{1} + \frac{e^{j\theta}}{U_N} \begin{bmatrix} M & N \end{bmatrix} \begin{bmatrix} p_G - j q_G \\ p_L - j q_L \end{bmatrix} \right) \tag{5.3}$$

that gives:

$$Mp_G + Np_L - j(Mp_G + Nq_L) = U_N e^{-j\theta}(e^{-j\varphi}u_G - U_N\mathbf{1}) \tag{5.4}$$

Therefore, the Gradient Projection procedure takes the iterative form

1.
$$\tilde{p}_G(t+1) = p_G(t) - \alpha\,\mathrm{Re}\{U_N e^{-j\theta}(e^{-j\varphi}u_G - U_N\mathbf{1})\} \tag{5.5}$$
$$\tilde{q}_G(t+1) = q_G(t) - \alpha\,\mathrm{Im}\{U_N e^{-j\theta}(e^{-j\varphi}u_G - U_N\mathbf{1})\} \tag{5.6}$$

2.
$$p_G(t+1) = \mathrm{proj}(\tilde{p}_G(t+1), \underline{p}, \overline{p}) \tag{5.7}$$
$$q_G(t+1) = \mathrm{proj}(\tilde{q}_G(t+1), \underline{q}, \overline{q}) \tag{5.8}$$

where

- $\mathrm{proj}(x, \underline{x}, \bar{x})$ is the component wise projection operator defined as

$$[\mathrm{proj}(x, \underline{x}, \overline{x})]_i = \begin{cases} x_i & \text{if } \underline{x}_i \le x_i \le \overline{x}_i \\ \underline{x}_i & \text{if } x_i < \underline{x}_i \\ \overline{x}_i & \text{if } x_i > \overline{x}_i \end{cases}$$

- α is a positive step size, which covers a fundamental role for the convergence of the algorithm.

The convergence, in fact, is a consequence of the following

Proposition 3. *If $f \ge 0\ \forall \begin{bmatrix} p_G^\top & q_G^\top \end{bmatrix}^\top$, if f is continuously differentiable and there exists a constant K such that*

$$\|\nabla f(p_G, q_G) - \nabla f(p_G + \Delta p_G, q_G + \Delta q_G)\| \le K\|\Delta\|, \quad \forall\, \Delta = \begin{bmatrix} \Delta p_G \\ \Delta q_G \end{bmatrix}$$

then, if $0 < \alpha < 2/K$ and f is convex, the sequence $\{p_G(t), q_G(t)\}$ generated by the gradient projection algorithm (5.5)-(5.8) converges to a point that minimizes f over the feasible set.

Proof. See [17] for the comprehensive proof. □

In our context, the two initial assumptions of the previous Proposition become:

1.
$$f = \frac{U_N^2}{2}\left(\begin{bmatrix} p_1 & p_G^\top & p_L^\top \end{bmatrix} X \begin{bmatrix} p_1 \\ p_G \\ p_L \end{bmatrix} + \begin{bmatrix} q_1 & q_G^\top & q_L^\top \end{bmatrix} X \begin{bmatrix} q_1 \\ q_G \\ q_L \end{bmatrix}\right) \ge 0$$

because X is symmetric positive definite;

2.

$$\begin{aligned}\|\nabla f(p_G, q_G) - \nabla f(p_G + \Delta p_G, q_G + \Delta q_G)\| &= \left\| \begin{bmatrix} M\Delta p_G \\ M\Delta q_G \end{bmatrix} \right\| \\ &= \left\| \begin{bmatrix} M & 0 \\ 0 & M \end{bmatrix} \begin{bmatrix} \Delta p_G \\ \Delta q_G \end{bmatrix} \right\| \leq \left\| \begin{bmatrix} M & 0 \\ 0 & M \end{bmatrix} \right\| \left\| \begin{bmatrix} \Delta p_G \\ \Delta q_G \end{bmatrix} \right\| \\ &= \rho(M) \left\| \begin{bmatrix} \Delta p_G \\ \Delta q_G \end{bmatrix} \right\|\end{aligned}$$

where $\rho(M)$ is the spectral radius and the last equivalence holds for the symmetry of M.

Then, it can be shown (see again [17]) that the following inequality holds:

$$f(p_G + \Delta p_G, q_G + \Delta q_G) \leq f(p_G, q_G) - \left(\frac{1}{\alpha} - \frac{K}{2}\right) \left\| \begin{bmatrix} \Delta p_G \\ \Delta q_G \end{bmatrix} \right\|^2$$

This result, together with the fact that f is bounded below, guarantees the convergence if the condition

$$\frac{1}{\alpha} - \frac{K}{2} > 0$$

is verified. Therefore, the step size must satisfy the inequality

$$\alpha < \frac{2}{K} = \frac{2}{\rho(M)}$$

6 Dual ascent approach

6.1 Only generators as agents

In this case, the scenario is perfectly comparable with that discussed in the previous chapter. By using the same initial propositions and results, we can state that, besides some positive multiplicative constants, our problem is equivalent to

$$\begin{aligned} \underset{p_G, q_G}{\text{minimize}} \quad & p_G^\top \frac{M}{2} p_G + p_L^\top N^\top p_G + q_G^\top \frac{M}{2} q_G + q_L^\top N^\top q_G && \text{(6.1a)} \\ \text{subject to} \quad & \underline{p}_i \leq p_i \leq \overline{p}_i && \text{(6.1b)} \\ & \underline{q}_i \leq q_i \leq \overline{q}_i \qquad i \in \mathcal{C} && \text{(6.1c)} \end{aligned}$$

with p_L and q_L that are fixed, but unknown.

As already discussed, the Lagrangian associated to (6.1) is

$$\begin{aligned} \mathcal{L}(p_G, p_L, q_G, q_L, \lambda_{\underline{p}}, \lambda_{\overline{p}}, \lambda_{\underline{q}}, \lambda_{\overline{q}}) = {} & p_G^\top \frac{M}{2} p_G + p_L^\top N^\top p_G + q_G^\top \frac{M}{2} q_G + q_L^\top N^\top q_G \\ & + \lambda_{\underline{p}}^\top (\underline{p} - p_G) + \lambda_{\overline{p}}^\top (p_G - \overline{p}) \\ & + \lambda_{\underline{q}}^\top (\underline{q} - q_G) + \lambda_{\overline{q}}^\top (q_G - \overline{q}) \end{aligned} \tag{6.2}$$

where we have introduced the vectors collecting the Lagrange multipliers for all the different constraints.

The dual ascent algorithm we are going to use consists in the iterative execution of the following alternating steps:

1. computation of the minimum with respect to the primal variables p_G and q_G

$$\tilde{p}_G(t+1) = \underset{p_G}{\operatorname{argmin}}\, \mathcal{L}(p_G, p_L, q_G(t), q_L, \lambda_{\underline{p}}(t), \lambda_{\overline{p}}(t), \lambda_{\underline{q}}(t), \lambda_{\overline{q}}(t)) \tag{6.3}$$

$$\tilde{q}_G(t+1) = \underset{q_G}{\operatorname{argmin}}\, \mathcal{L}(p_G(t), p_L, q_G, q_L, \lambda_{\underline{p}}(t), \lambda_{\overline{p}}(t), \lambda_{\underline{q}}(t), \lambda_{\overline{q}}(t)) \quad (6.4)$$

The closed form is easily obtainable: by imposing

$$\frac{\partial}{\partial p_G}\mathcal{L}(\dots) = Mp_G + Np_L - \lambda_{\underline{p}}(t) + \lambda_{\overline{p}}(t)$$

to be equal to zero, we have

$$\tilde{p}_G(t+1) = M^{-1}(\lambda_{\underline{p}}(t) - \lambda_{\overline{p}}(t) - Np_L) \quad (6.5)$$

Similarly, the update for the reactive power becomes:

$$\tilde{q}_G(t+1) = M^{-1}(\lambda_{\underline{q}}(t) - \lambda_{\overline{q}}(t) - Nq_L) \quad (6.6)$$

2. update of the Lagrangian multipliers

$$\lambda_{\underline{p}}(t+1) = \left[\lambda_{\underline{p}}(t) + \gamma_{\lambda_{\underline{p}}} \frac{\partial \mathcal{L}(\tilde{p}_G(t+1), p_L, \tilde{q}_G(t+1), q_L, \lambda_{\underline{p}}, \lambda_{\overline{p}}(t), \lambda_{\underline{q}}(t), \lambda_{\overline{q}}(t))}{\partial \lambda_{\underline{p}}}\right]_+$$

$$\lambda_{\overline{p}}(t+1) = \left[\lambda_{\overline{p}}(t) + \gamma_{\lambda_{\overline{p}}} \frac{\partial \mathcal{L}(\tilde{p}_G(t+1), p_L, \tilde{q}_G(t+1), q_L, \lambda_{\underline{p}}(t), \lambda_{\overline{p}}, \lambda_{\underline{q}}(t), \lambda_{\overline{q}}(t))}{\partial \lambda_{\overline{p}}}\right]_+$$

$$\lambda_{\underline{q}}(t+1) = \left[\lambda_{\underline{q}}(t) + \gamma_{\lambda_{\underline{q}}} \frac{\partial \mathcal{L}(\tilde{p}_G(t+1), p_L, \tilde{q}_G(t+1), q_L, \lambda_{\underline{p}}(t), \lambda_{\overline{p}}(t), \lambda_{\underline{q}}, \lambda_{\overline{q}}(t))}{\partial \lambda_{\underline{q}}}\right]_+$$

$$\lambda_{\overline{q}}(t+1) = \left[\lambda_{\overline{q}}(t) + \gamma_{\lambda_{\overline{q}}} \frac{\partial \mathcal{L}(\tilde{p}_G(t+1), p_L, \tilde{q}_G(t+1), q_L, \lambda_{\underline{p}}(t), \lambda_{\overline{p}}(t), \lambda_{\underline{q}}(t), \lambda_{\overline{q}})}{\partial \lambda_{\overline{q}}}\right]_+$$

where

- $\gamma_{\lambda_{\underline{p}}}$, $\gamma_{\lambda_{\overline{p}}}$, $\gamma_{\lambda_{\underline{q}}}$ and $\gamma_{\lambda_{\overline{q}}}$ are suitable positive constants a-priori assigned;
- $[\cdot]_+$ is the operator corresponding to the projection onto the positive orthant;

For what concerns, for example, $\lambda_{\underline{p}}(t+1)$, we have that

$$\frac{\partial}{\partial \lambda_{\underline{p}}}\mathcal{L}(\tilde{p}_G(t+1), p_L, \tilde{q}_G(t+1), q_L, \lambda_{\underline{p}}, \lambda_{\overline{p}}(t), \lambda_{\underline{q}}(t), \lambda_{\overline{q}}(t))$$
$$= \underline{p} - \tilde{p}_G(t+1) = \underline{p} - M^{-1}(\lambda_{\underline{p}}(t) - \lambda_{\overline{p}}(t) - Np_L)$$

obtaining

$$\begin{aligned}\lambda_{\underline{p}}(t+1) &= [\lambda_{\underline{p}}(t) + \gamma_{\lambda_{\underline{p}}}[\underline{p} - M^{-1}(\lambda_{\underline{p}}(t) - \lambda_{\overline{p}}(t) - Np_L)]]_+ \\ &= [(I - \gamma_{\lambda_{\underline{p}}} M^{-1})\lambda_{\underline{p}}(t) + \gamma_{\lambda_{\underline{p}}}(M^{-1}\lambda_{\overline{p}}(t) + \underline{p} + M^{-1}Np_L)]_+\end{aligned}$$

In a similar way we have:

$$\begin{aligned}\lambda_{\overline{p}}(t+1) &= [\lambda_{\overline{p}}(t) + \gamma_{\lambda_{\overline{p}}}(\tilde{p}_G(t+1) - \overline{p})]_+ \\ &= [(I - \gamma_{\lambda_{\overline{p}}} M^{-1})\lambda_{\overline{p}}(t) + \gamma_{\lambda_{\overline{p}}}(M^{-1}\lambda_{\underline{p}}(t) - \overline{p} - M^{-1}Np_L)]_+ \\ \lambda_{\underline{q}}(t+1) &= [\lambda_{\underline{q}}(t) + \gamma_{\lambda_{\underline{p}}}(\underline{q} - \tilde{q}_G(t+1))]_+ \\ &= [(I - \gamma_{\lambda_{\underline{q}}} M^{-1})\lambda_{\underline{q}}(t) + \gamma_{\lambda_{\underline{q}}}(M^{-1}\lambda_{\overline{q}}(t) + \underline{q} + M^{-1}Np_L)]_+ \\ \lambda_{\overline{q}}(t+1) &= [\lambda_{\overline{q}}(t) + \gamma_{\lambda_{\overline{q}}}(\tilde{q}_G(t+1) - \overline{q})]_+ \\ &= [(I - \gamma_{\lambda_{\overline{q}}} M^{-1})\lambda_{\overline{q}}(t) + \gamma_{\lambda_{\overline{q}}}(M^{-1}\lambda_{\underline{q}}(t) - \overline{q} - M^{-1}Np_L)]_+\end{aligned}$$

3. projection of the primal variables into the feasible set

$$p_G(t+1) = \text{proj}(\tilde{p}_G(t+1), \underline{p}, \overline{p}) \tag{6.7}$$

$$q_G(t+1) = \text{proj}(\tilde{q}_G(t+1), \underline{q}, \overline{q}) \tag{6.8}$$

The parameters γ's cover an important role for the convergence of the algorithm. In this sense, as proved in [12], they must satisfy the condition

$$\gamma_{\lambda_{\underline{p}}}, \gamma_{\lambda_{\overline{p}}}, \gamma_{\lambda_{\underline{q}}}, \gamma_{\lambda_{\overline{p}}} < \frac{2}{\rho(M^{-1})}$$

For what concerns the update of the dual variables, it has been proposed a double version of each update: the first one is the expression that will be actually used in the implementation of the algorithm, the second one underlines the independence of the dual variables on the primal ones.

Notice that the above algorithm differs from the standard dual ascent one in the third step, when the projection on the feasible set occurs. However they are equivalent, because:

- the minimization of the primal variables (step 1) is identical for both standard and modified dual ascent algorithm;
- the update of the dual variables (step 2) is based on the value of the primal variable calculated at step 1, when it is still not constrained, which implies the independence of the dual variables on the primal ones as just seen.

It means that, if we run in parallel the standard and modified version of the dual ascent algorithm with the same initial values for both primal and dual variables, then their evolutions are identical at every time.

These equations make use of the information about the active and reactive powers required by the loads: in our contest, however, the only smart agents are represented by the generators. Our goal is to re-write these physical quantities in terms of measurable variables.

From Proposition 2 in Chapter 5, we have:

$$\begin{bmatrix} u_1 \\ u_G \\ u_L \end{bmatrix} \approx e^{j\varphi}\left(U_N\mathbf{1} + \frac{e^{j\theta}}{U_N}\begin{bmatrix} 0 & \mathbf{0} & \mathbf{0} \\ \mathbf{0} & M & N \\ \mathbf{0} & N^\top & O \end{bmatrix}\begin{bmatrix} 0 \\ \bar{s}_G \\ \bar{s}_L \end{bmatrix}\right)$$

and in particular

$$u_G \approx e^{j\varphi}\left(U_N\mathbf{1} + \frac{e^{j\theta}}{U_N}\begin{bmatrix} \mathbf{0} & M & N \end{bmatrix}\begin{bmatrix} 0 \\ \bar{s}_G \\ \bar{s}_L \end{bmatrix}\right) = e^{j\varphi}\left(U_N\mathbf{1} + \frac{e^{j\theta}}{U_N}(M\bar{s}_G + N\bar{s}_L)\right)$$

Then, by forgetting the approximation for an easier notation, we have

$$N\bar{s}_L = e^{-j\theta}U_N(e^{-j\varphi}u_G - U_N\mathbf{1}) - M\bar{s}_G$$

obtaining

$$\begin{cases} Np_L = U_N(\mathrm{Re}\{u_G e^{-j(\theta+\varphi)}\} - U_N\cos\theta\mathbf{1}) - Mp_G \\ Nq_L = -U_N(\mathrm{Im}\{u_G e^{-j(\theta+\varphi)}\} + U_N\sin\theta\mathbf{1}) - Mq_G \end{cases}$$

Therefore, by denoting with $u_G(t)$ the generator complex voltages after power $p_G(t)+jq_G(t)$ have been applied, updates (6.5) and (6.6) take the form:

$$\tilde{p}_G(t+1) = M^{-1}\big(\lambda_{\underline{p}}(t) - \lambda_{\overline{p}}(t) - U_N(\mathrm{Re}\{u_G(t)e^{-j(\theta+\varphi)}\} - U_N\cos\theta\mathbf{1})\big) + p_G(t)$$

$$\tilde{q}_G(t+1) = M^{-1}\big(\lambda_{\underline{q}}(t) - \lambda_{\overline{q}}(t) + U_N(\mathrm{Im}\{u_G(t)e^{-j(\theta+\varphi)}\} + U_N\sin\theta\mathbf{1})\big) + q_G(t)$$

At this point, the dependence is only on the voltages and the power injections of the generators. The next step is to show that, for every generator, the decision is dependent only on local quantities, that are the voltages of its neighbours. With this aim, we provide the following

Lemma 2. *There exists a unique symmetric matrix $G \in \mathbb{R}^{m\times m}$ satisfying the conditions*

$$\begin{cases} \begin{bmatrix} 0 & \mathbf{0} \\ \mathbf{0} & M \end{bmatrix} G = I - \mathbf{1}\mathbf{1}_0^\top \\ G\mathbf{1} = 0 \end{cases} \tag{6.9}$$

Proof. With simple calculations, we have that the following matrix satisfies the conditions

$$G = \begin{bmatrix} \mathbf{1}^\top M^{-1}\mathbf{1} & -\mathbf{1}^\top M^{-1} \\ -M^{-1}\mathbf{1} & M^{-1} \end{bmatrix}$$

The uniqueness can be shown as in the proof of Lemma 1. □

The importance of the matrix G just introduced concerns its sparsity pattern, stated by the following

Lemma 3. *The sparsity pattern of the matrix G is*

$$G_{ij} \neq 0 \quad \Leftrightarrow \quad j \in \mathcal{N}(i) \cup \{i\}$$

Proof. See [11]. □

It is now clear that the following chain of equations holds:

$$\begin{aligned}
\tilde{p}_G(t+1) &= M^{-1}\big(\lambda_{\underline{p}}(t) - \lambda_{\overline{p}}(t) - U_N(\mathrm{Re}\{u_G(t)e^{-j(\theta+\varphi)}\} - U_N\cos\theta\mathbf{1})\big) + p_G(t) \\
&= G_{\lrcorner}\big(\lambda_{\underline{p}}(t) - \lambda_{\overline{p}}(t) - U_N(\mathrm{Re}\{u_G(t)e^{-j(\theta+\varphi)}\} - U_N\cos\theta\mathbf{1})\big) + p_G(t) \\
&= G_{\llcorner\lrcorner}\left(\begin{bmatrix} 0 \\ \lambda_{\underline{p}}(t) - \lambda_{\overline{p}}(t) - U_N(\mathrm{Re}\{u_G(t)e^{-j(\theta+\varphi)}\} - U_N\cos\theta\mathbf{1}) \end{bmatrix}\right) + p_G(t)
\end{aligned} \tag{6.10}$$

where $G_{\llcorner\lrcorner}$ is G without the first row and $G_{\lrcorner}$ is G without the first row and the first column.

The last equation is component-wise equivalent to

$$\begin{aligned}
\tilde{p}_G(t+1)_i = p_G(t)_i + \\
\sum_{j\in\mathcal{N}\cup\{i\}\setminus\{1\}} G_{ij}\Big(\lambda_{\underline{p}}(t)_j - \lambda_{\overline{p}}(t)_j - U_N[|u|_j\cos(\angle u_j - \theta - \varphi) - U_N\cos\theta]\Big)
\end{aligned} \tag{6.11}$$

and similarly

$$\begin{aligned}
\tilde{q}_G(t+1)_i = q_G(t)_i + \\
\sum_{j\in\mathcal{N}\cup\{i\}\setminus\{1\}} G_{ij}\Big(\lambda_{\underline{q}}(t)_j - \lambda_{\overline{q}}(t)_j + U_N[|u|_j\sin(\angle u_j - \theta - \varphi) + U_N\sin\theta]\Big)
\end{aligned} \tag{6.12}$$

Now, for what concerns the active powers, we have:

1. $$\sum_{j\in\mathcal{N}\cup\{i\}\setminus\{1\}} G_{ij}\Big(\lambda_{\underline{p}}(t)_j - \lambda_{\overline{p}}(t)_j\Big) = \sum_{j\in\mathcal{N}\cup\{i\}} G_{ij}\Big(\lambda_{\underline{p}}(t)_j - \lambda_{\overline{p}}(t)_j\Big)$$

   because, as suggested in Equation (6.10), we have imposed $\lambda_{\underline{p}}(t)_1 = \lambda_{\overline{p}}(t)_1 = 0$ for the PCC.

2. $$\begin{aligned}
   &\sum_{j\in\mathcal{N}\cup\{i\}\setminus\{1\}} G_{ij}\Big(|u|_j\cos(\angle u_j - \theta - \varphi) - U_N\cos\theta\Big) \\
   &= \sum_{j\in\mathcal{N}\cup\{i\}\setminus\{1\}} G_{ij}\Big(|u|_j\cos(\angle u_j - \theta - \varphi)\Big) - U_N\cos\theta \sum_{j\in\mathcal{N}\cup\{i\}\setminus\{1\}} G_{ij} \\
   &= \sum_{j\in\mathcal{N}\cup\{i\}} G_{ij}\Big(|u|_j\cos(\angle u_j - \theta - \varphi)\Big)
   \end{aligned}$$

because, for condition 2 in Lemma 2 and for Lemma 3, we have

$$\begin{aligned} &- U_N \cos\theta \sum_{j \in \mathcal{N} \cup \{i\} \setminus \{1\}} G_{ij} \\ &= U_N \cos\theta G_{i1} = G_{i1} |u_1| \cos(\angle u_1 - \theta - \varphi) \end{aligned}$$

Following the same steps also for the reactive power updates, we obtain the simpler expressions:

$$\tilde{p}_G(t+1)_i = p_G(t)_i + \sum_{j \in \mathcal{N} \cup \{i\}} G_{ij} \Big(\lambda_{\underline{p}}(t)_j - \lambda_{\overline{p}}(t)_j - U_N |u|_j \cos(\angle u_j - \theta - \varphi) \Big) \tag{6.13}$$

$$\tilde{q}_G(t+1)_i = q_G(t)_i + \sum_{j \in \mathcal{N} \cup \{i\}} G_{ij} \Big(\lambda_{\underline{q}}(t)_j - \lambda_{\overline{q}}(t)_j + U_N |u|_j \sin(\angle u_j - \theta - \varphi) \Big) \tag{6.14}$$

Notice that now the updates are only dependent on the voltages of the neighbours and of the PCC. Then, we have finally obtained a distributed algorithm, for which only communication between neighbouring agents is needed: in fact, as said in section 3.1.3, in the power system analysis, node 1 is a slack bus with fixed voltage magnitude and angle. The knowledge about the PCC voltage can then be achieved by each node at the connection to the grid, when also the construction of the neighbours set and the estimation of the local grid parameters take place [11].

We can finally summarize the whole algorithm.

6.1.1 Only generators as agents algorithm

Let all generators (except the PCC: $\mathcal{A} \equiv \mathcal{C} \setminus \{1\}$) store the dual variables $\lambda_{\underline{p}}$, $\lambda_{\overline{p}}$, $\lambda_{\underline{q}}$, $\lambda_{\overline{p}}$ and the positive scalar parameters $\gamma_{\lambda_{\underline{p}}}$, $\gamma_{\lambda_{\overline{p}}}$, $\gamma_{\lambda_{\underline{q}}}$, $\gamma_{\lambda_{\overline{q}}}$. Let θ be the impedance angle defined in assumption 2 in section 3.1.2, and $\underline{p}$, $\overline{p}$, $\underline{q}$, $\overline{q}$ the lower and upper bounds for active and reactive powers, respectively. Let G the matrix introduced in Lemma 2. At every synchronous iteration, each node i except the PCC executes the following ordered operations:

1. measures its own voltage and gathers the voltage measurements and the Lagrange multipliers from its neighbours

$$\{u_k \in \mathbb{C} \ , \ \lambda_{\underline{p}_k}, \lambda_{\overline{p}_k}, \lambda_{\underline{q}_k}, \lambda_{\overline{q}_k} \in \mathbb{R}_+ \ , \ k \in \mathcal{N}(i) \cup \{i\}\}$$

2. computes the optimal active and reactive power, without taking in consideration the generation limits

$$\tilde{p}_i \leftarrow p_i + \sum_{j \in \mathcal{N} \cup \{i\}} G_{ij} \Big(\lambda_{\underline{p}_j} - \lambda_{\overline{p}_j} - U_N |u|_j \cos(\angle u_j - \theta - \varphi) \Big) \tag{6.15}$$

$$\tilde{q}_i \leftarrow q_i + \sum_{j \in \mathcal{N} \cup \{i\}} G_{ij} \Big(\lambda_{\underline{q}_j} - \lambda_{\overline{q}_j} + U_N |u|_j \sin(\angle u_j - \theta - \varphi) \Big) \tag{6.16}$$

3. updates the dual variables

$$\lambda_{\underline{p}_i} \leftarrow [\lambda_{\underline{p}_i} + \gamma_{\lambda_{\underline{p}}} (\underline{p}_i - \tilde{p}_i)]_+ \tag{6.17}$$

$$\lambda_{\overline{p}_i} \leftarrow [\lambda_{\overline{p}_i} + \gamma_{\lambda_{\overline{p}}} (\tilde{p}_i - \overline{p}_i)]_+ \tag{6.18}$$

$$\lambda_{\underline{q}_i} \leftarrow [\lambda_{\underline{q}_i} + \gamma_{\lambda_{\underline{q}}} (\underline{q}_i - \tilde{q}_i)]_+ \tag{6.19}$$

$$\lambda_{\overline{q}_i} \leftarrow [\lambda_{\overline{q}_i} + \gamma_{\lambda_{\overline{q}}} (\tilde{q}_i - \overline{q}_i)]_+ \tag{6.20}$$

4. projects the complex power into the feasible set

$$p_i \leftarrow \text{proj}(\tilde{p}_i, \underline{p}_i, \overline{p}_i) \tag{6.21}$$

$$q_i \leftarrow \text{proj}(\tilde{q}_i, \underline{q}_i, \overline{q}_i) \tag{6.22}$$

6.2 Both generators and loads as agents

We now propose a second version of the dual ascent algorithm, in which all the nodes, included the loads, have computational and sensing capabilities. It represents a sort of connection between the previous approach and the next one.

We now briefly see how the steps taken so far fit in this new configuration.

First of all, by adopting the block decomposition

$$u = \begin{bmatrix} u_1 \\ u_{\text{in}} \end{bmatrix} \quad , \quad s = p + jq = \begin{bmatrix} p_1 + jq_1 \\ p_{\text{in}} + jq_{\text{in}} \end{bmatrix}$$

where the subscript $_{\text{in}}$ denotes the set of all the *internal nodes*, i.e. all the nodes except the PCC, the matrix X of Lemma 1 assumes the structure

$$X = \begin{bmatrix} 0 & \mathbf{0} \\ \mathbf{0} & M \end{bmatrix} \quad , \quad M \in \mathbb{R}^{(n-1)\times(n-1)}$$

The cost function written in terms of p_{in} and q_{in} is

$$\bar{u}^\top L u \approx \frac{p^\top X p}{U_N^2} + \frac{q^\top X q}{U_N^2} = \frac{p_{\text{in}}^\top M p_{\text{in}}}{U_N^2} + \frac{q_{\text{in}}^\top M q_{\text{in}}}{U_N^2} \tag{6.23}$$

obtaining, again besides some positive multiplicative constants, the equivalent problem

$$\underset{p_{\text{in}},q_{\text{in}}}{\text{minimize}} \quad p_{\text{in}}^\top \frac{M}{2} p_{\text{in}} + q_{\text{in}}^\top \frac{M}{2} q_{\text{in}} \tag{6.24a}$$

$$\text{subject to} \quad \underline{p}_i \le p_i \le \overline{p}_i \tag{6.24b}$$

$$\underline{q}_i \le q_i \le \overline{q}_i \qquad i \in \mathcal{V} \tag{6.24c}$$

In this problem, inequalities (6.24b) and (6.24c) are actual lower and upper bounds on injection capabilities if node i is a generator, while are reduced to equalities if i is a load (with $\underline{p}_i = \overline{p}_i$ and $\underline{q}_i = \overline{q}_i$, equal to the opposite of the i-th power demand).

The Lagrangian associated to (6.24) is

$$\begin{aligned}\mathcal{L}(p_{\text{in}}, q_{\text{in}}, \lambda_{\underline{p}}, \lambda_{\overline{p}}, \lambda_{\underline{q}}, \lambda_{\overline{q}}) = p_{\text{in}}^\top \frac{M}{2} p_{\text{in}} + q_{\text{in}}^\top \frac{M}{2} q_{\text{in}} + \lambda_{\underline{p}}^\top (\underline{p} - p_{\text{in}}) + \lambda_{\overline{p}}^\top (p_{\text{in}} - \overline{p}) \\ + \lambda_{\underline{q}}^\top (\underline{q} - q_{\text{in}}) + \lambda_{\overline{q}}^\top (q_{\text{in}} - \overline{q})\end{aligned} \tag{6.25}$$

and the dual ascent algorithm consists in the following alternating steps:

1. computation of the minimum with respect to the primal variables p_{in} and q_{in}

$$\tilde{p}_{\text{in}}(t+1) = \underset{p_{\text{in}}}{\text{argmin}}\ \mathcal{L}(p_{\text{in}}, q_{\text{in}}(t), \lambda_{\underline{p}}(t), \lambda_{\overline{p}}(t), \lambda_{\underline{q}}(t), \lambda_{\overline{q}}(t)) \tag{6.26}$$

$$\tilde{q}_{\text{in}}(t+1) = \underset{q_{\text{in}}}{\text{argmin}}\ \mathcal{L}(p_{\text{in}}(t), q_{\text{in}}, \lambda_{\underline{p}}(t), \lambda_{\overline{p}}(t), \lambda_{\underline{q}}(t), \lambda_{\overline{q}}(t)) \tag{6.27}$$

   The closed form is easily obtainable: by imposing

$$\frac{\partial}{\partial p_{\text{in}}} \mathcal{L}(p_{\text{in}}, q_{\text{in}}(t), \lambda_{\underline{p}}(t), \lambda_{\overline{p}}(t), \lambda_{\underline{q}}(t), \lambda_{\overline{q}}(t)) = M p_{\text{in}} - \lambda_{\underline{p}}(t) + \lambda_{\overline{p}}(t)$$

   to be equal to zero, we have

$$\tilde{p}_{\text{in}}(t+1) = M^{-1}(\lambda_{\underline{p}}(t) - \lambda_{\overline{p}}(t))$$

   Similarly, the update for the reactive power becomes:

$$\tilde{q}_{\text{in}}(t+1) = M^{-1}(\lambda_{\underline{q}}(t) - \lambda_{\overline{q}}(t))$$

2. update of the Lagrangian multipliers

$$\lambda_{\underline{p}}(t+1) = \left[\lambda_{\underline{p}}(t) + \gamma_{\lambda_{\underline{p}}} \frac{\partial \mathcal{L}(\tilde{p}_{\text{in}}(t+1), \tilde{q}_{\text{in}}(t+1), \lambda_{\underline{p}}, \lambda_{\overline{p}}(t), \lambda_{\underline{q}}(t), \lambda_{\overline{q}}(t))}{\partial \lambda_{\underline{p}}}\right]_+$$

$$\lambda_{\overline{p}}(t+1) = \left[\lambda_{\overline{p}}(t) + \gamma_{\lambda_{\overline{p}}} \frac{\partial \mathcal{L}(\tilde{p}_{\text{in}}(t+1), \tilde{q}_{\text{in}}(t+1), \lambda_{\underline{p}}(t), \lambda_{\overline{p}}, \lambda_{\underline{q}}(t), \lambda_{\overline{q}}(t))}{\partial \lambda_{\overline{p}}}\right]_+$$

$$\lambda_{\underline{q}}(t+1) = \left[\lambda_{\underline{q}}(t) + \gamma_{\lambda_{\underline{q}}} \frac{\partial \mathcal{L}(\tilde{p}_{\text{in}}(t+1), \tilde{q}_{\text{in}}(t+1), \lambda_{\underline{p}}(t), \lambda_{\overline{p}}(t), \lambda_{\underline{q}}, \lambda_{\overline{q}}(t))}{\partial \lambda_{\underline{q}}}\right]_+$$

$$\lambda_{\overline{q}}(t+1) = \left[\lambda_{\overline{q}}(t) + \gamma_{\lambda_{\overline{q}}} \frac{\partial \mathcal{L}(\tilde{p}_{\text{in}}(t+1), \tilde{q}_{\text{in}}(t+1), \lambda_{\underline{p}}(t), \lambda_{\overline{p}}(t), \lambda_{\underline{q}}(t), \lambda_{\overline{q}})}{\partial \lambda_{\overline{q}}}\right]_+$$

For what concerns, for example, $\lambda_{\underline{p}}(t+1)$, we have that

$$\frac{\partial}{\partial \lambda_{\underline{p}}} \mathcal{L}(\tilde{p}_{\text{in}}(t+1), \tilde{q}_{\text{in}}(t+1), \lambda_{\underline{p}}, \lambda_{\overline{p}}(t), \lambda_{\underline{q}}(t), \lambda_{\overline{q}}(t)) = \underline{p} - \tilde{p}_{\text{in}}(t+1) = \underline{p} - M^{-1}(\lambda_{\underline{p}}(t) - \lambda_{\overline{p}}(t))$$

obtaining

$$\lambda_{\underline{p}}(t+1) = [\lambda_{\underline{p}}(t) + \gamma_{\lambda_{\underline{p}}}[\underline{p} - M^{-1}(\lambda_{\underline{p}}(t) - \lambda_{\overline{p}}(t))]]_+$$

In a similar way we have:

$$\lambda_{\overline{p}}(t+1) = [\lambda_{\overline{p}}(t) + \gamma_{\lambda_{\overline{p}}}(\tilde{p}_{\text{in}}(t+1) - \overline{p})]_+$$

$$\lambda_{\underline{q}}(t+1) = [\lambda_{\underline{q}}(t) + \gamma_{\lambda_{\underline{p}}}(\underline{q} - \tilde{q}_{\text{in}}(t+1))]_+$$

$$\lambda_{\overline{q}}(t+1) = [\lambda_{\overline{q}}(t) + \gamma_{\lambda_{\overline{q}}}(\tilde{q}_{\text{in}}(t+1) - \overline{q})]_+$$

3. projection of the primal variable into the feasible set

$$p_{\text{in}}(t+1) = \text{proj}(\tilde{p}_{\text{in}}(t+1), \underline{p}, \overline{p}) \tag{6.28}$$

$$q_{\text{in}}(t+1) = \text{proj}(\tilde{q}_{\text{in}}(t+1), \underline{q}, \overline{q}) \tag{6.29}$$

At this point, by denoting with $Y_{\lrcorner}$ the matrix obtained by removing the first row and column of Y and with $Y_{\llcorner\lrcorner}$ removing only the first row, thanks to Lemma 1 we have:

$$M^{-1}(\lambda_{\underline{p}} - \lambda_{\overline{p}}) = Y_{\lrcorner}(\lambda_{\underline{p}} - \lambda_{\overline{p}}) = Y_{\llcorner\lrcorner} \begin{bmatrix} 0 \\ \lambda_{\underline{p}} - \lambda_{\overline{p}} \end{bmatrix}$$

that from a component wise point of view is equivalent to, for $i \in \mathcal{V} \setminus \{1\}$

$$[M^{-1}(\lambda_{\underline{p}} - \lambda_{\overline{p}})]_i = \sum_{j \in \mathcal{N}(i) \cup \{i\}} Y_{ij}(\lambda_{\underline{p}_j} - \lambda_{\overline{p}_j}) \tag{6.30}$$

with $\lambda_{\underline{p}_1} = \lambda_{\overline{p}_1} = 0$ as states in (6.2).

We can finally summarize the whole algorithm.

6.2.1 Both generators and loads as agents algorithm

Let all nodes store the dual variables $\lambda_{\underline{p}}$, $\lambda_{\overline{p}}$, $\lambda_{\underline{q}}$, $\lambda_{\overline{p}}$ and the positive scalar parameters $\gamma_{\lambda_{\underline{p}}}$, $\gamma_{\lambda_{\overline{p}}}$, $\gamma_{\lambda_{\underline{q}}}$, $\gamma_{\lambda_{\overline{q}}}$. Let θ be the impedance angle defined in assumption 2 in subsection 3.1.2, and $\underline{p}$, $\overline{p}$, $\underline{q}$, $\overline{q}$ the lower and upper bounds for active and reactive powers, respectively. Let Y the real-valued Laplacian of the grid model. At every synchronous iteration, each node i except the PCC executes the following ordered operations:

1. gathers the Lagrange multipliers from its neighbours

$$\{\lambda_{\underline{p}_k}, \lambda_{\overline{p}_k}, \lambda_{\underline{q}_k}, \lambda_{\overline{q}_k} \in \mathbb{R}_+ \ , \ k \in \mathcal{N}(i) \cup \{i\}\}$$

2. computes the optimal active and reactive power, without taking in consideration the generation limits

$$\tilde{p}_i \leftarrow \sum_{j \in \mathcal{N}(i) \cup \{i\}} Y_{ij}(\lambda_{\underline{p}_i} - \lambda_{\overline{p}_i}) \tag{6.31}$$

$$\tilde{q}_i \leftarrow \sum_{j \in \mathcal{N}(i) \cup \{i\}} Y_{ij}(\lambda_{\underline{q}_i} - \lambda_{\overline{q}_i}) \tag{6.32}$$

3. updates the dual variables

$$\lambda_{\underline{p}_i} \leftarrow [\lambda_{\underline{p}_i} + \gamma_{\lambda_{\underline{p}}}(\underline{p}_i - \tilde{p}_i)]_+ \tag{6.33}$$

$$\lambda_{\overline{p}_i} \leftarrow [\lambda_{\overline{p}_i} + \gamma_{\lambda_{\overline{p}}}(\tilde{p}_i - \overline{p}_i)]_+ \tag{6.34}$$

$$\lambda_{\underline{q}_i} \leftarrow [\lambda_{\underline{q}_i} + \gamma_{\lambda_{\underline{q}}}(\underline{q}_i - \tilde{q}_i)]_+ \tag{6.35}$$

$$\lambda_{\overline{q}_i} \leftarrow [\lambda_{\overline{q}_i} + \gamma_{\lambda_{\overline{q}}}(\tilde{q}_i - \overline{q}_i)]_+ \tag{6.36}$$

4. projects the complex power into the feasible set

$$p_i \leftarrow \text{proj}(\tilde{p}_i, \underline{p}_i, \overline{p}_i) \tag{6.37}$$

$$q_i \leftarrow \text{proj}(\tilde{q}_i, \underline{q}_i, \overline{q}_i) \tag{6.38}$$

7

ADMM approach

We now propose a distributed iterative algorithm in order to solve (7.5). It can be considered distributed because each node needs to communicate only with its neighbours and keeps in memory only a copy of its own state and copies of the states of its neighbours. The copy of state x_j stored in memory by node i is referred to as $x_j^{(i)}$. Assume also that local edge variables are available: it means that for the edge connecting nodes i and j there exists a variable $z^{(i,j)}$ containing copies only of the states of i and j.

Recall now Equation (3.4): it states that the complex power corresponding to node i is

$$s_i = u_i \bar{i}_i$$

with $p_i = \mathrm{Re}\{s_i\} > 0$ for generators and $p_i < 0$ for loads. For the conservation of energy, it is clear that the sum of the (positive) active powers injected by the generators and the (negative) active powers injected by the loads, i.e. the difference of the active power injections by the generators and the active power consumptions by the loads, is equal to the total line power losses (this equivalence is formally proved in A.2). Therefore, we can equivalently say the objective is to minimize the quantity

$$\sum_{i \in \mathcal{V}} p_i \ .$$

In this scenario, the general problem (4.2) takes the form:

$$\begin{aligned}
\text{minimize} \quad & \sum_{i \in \mathcal{V}} p_i && \text{(7.1a)} \\
\text{subject to} \quad & p_i + j q_i = u_i e^{j\theta} Y^i \bar{u} && \text{(7.1b)} \\
& \underline{p}_i \leq p_i \leq \bar{p}_i && \text{(7.1c)} \\
& \underline{q}_i \leq q_i \leq \bar{q}_i && \text{(7.1d)}
\end{aligned}$$

where Y^i denotes the i-th row of Y.

In particular, we are interested in considering the $N \times 1$ vector of complex voltages u as a $2N \times 1$ vector containing real and imaginary components

$$X = \begin{bmatrix} u_{1_{\mathrm{Re}}} \\ u_{1_{\mathrm{Im}}} \\ u_{2_{\mathrm{Re}}} \\ u_{2_{\mathrm{Im}}} \\ \vdots \end{bmatrix} \in \mathbb{R}^{2N}$$

As shown in Appendix A, we can write

$$\begin{aligned} p_i &= X^\top \begin{bmatrix} \mathbf{1}_{2i-1} & \mathbf{1}_{2i} \end{bmatrix} \begin{bmatrix} \cos\theta & \sin\theta \\ -\sin\theta & \cos\theta \end{bmatrix} \begin{bmatrix} Y^i & 0 \\ 0 & Y^i \end{bmatrix} \begin{bmatrix} I_N \otimes \begin{bmatrix} 1 & 0 \end{bmatrix} \\ I_N \otimes \begin{bmatrix} 0 & 1 \end{bmatrix} \end{bmatrix} X \\ &=: X^\top P_i X = p_i(X) \end{aligned} \tag{7.2}$$

In a similar way it is possible to write q_i as:

$$\begin{aligned} q_i &= X^\top \begin{bmatrix} \mathbf{1}_{2i-1} & \mathbf{1}_{2i} \end{bmatrix} \begin{bmatrix} \sin\theta & -\cos\theta \\ \cos\theta & \sin\theta \end{bmatrix} \begin{bmatrix} Y^i & 0 \\ 0 & Y^i \end{bmatrix} \begin{bmatrix} I_N \otimes \begin{bmatrix} 1 & 0 \end{bmatrix} \\ I_N \otimes \begin{bmatrix} 0 & 1 \end{bmatrix} \end{bmatrix} X \\ &=: X^\top Q_i X = q_i(X) \end{aligned} \tag{7.3}$$

With these considerations, problem (7.1) can be rewritten as

$$\underset{X}{\text{minimize}} \quad \sum_{i \in \mathcal{V}} p_i(X) \tag{7.4a}$$

$$\text{subject to} \quad \underline{p}_i \leq p_i(X) \leq \bar{p}_i \tag{7.4b}$$

$$\underline{q}_i \leq q_i(X) \leq \bar{q}_i \tag{7.4c}$$

By considering again Equation (7.1b), we can state that the complex power corresponding to node i is function only of the voltages of node i itself and of all the other nodes j which are electrically connected to node i: in fact, the element j of the row Y^i is non-zero only if there exists an edge connecting node i to node j.

In this sense, problem (7.4) can take a form that underlines the local dependences, as the following:

$$\underset{X^i \in \mathcal{C}_i}{\text{minimize}} \quad \sum_{i \in \mathcal{V}} p_i(X^i) \tag{7.5}$$

in which X^i is defined as

$$X^i = \begin{bmatrix} x_i \\ \{x_j\}_{j \in \mathcal{N}(i)} \end{bmatrix} \in \mathbb{R}^{2|N(i)|+2} \quad , \quad x_k = \begin{bmatrix} u_{\mathrm{Re}_k} \\ u_{\mathrm{Im}_k} \end{bmatrix} \in \mathbb{R}^2$$

and $\mathcal{C}_i$ is the set of feasible points satisfying (7.4b) and (7.4c). See Appendix A.2 for the details.

In the classical ADMM scenario, problem (7.5) is formulated as follows:

$$\begin{aligned}
\underset{X^{(i)}\in\mathcal{C}_i}{\text{minimize}} \quad & \sum_{i\in\mathcal{V}} p_i(X^{(i)}) && \text{(7.6a)}\\
\text{subject to} \quad & x_i^{(i)} = z_i^{(i,j)},\ x_j^{(i)} = z_j^{(i,j)} && \text{(7.6b)}\\
& x_i^{(i)} = z_i^{(j,i)},\ x_j^{(i)} = z_j^{(j,i)} \qquad \forall j \in \mathcal{N}(i) && \text{(7.6c)}
\end{aligned}$$

where

$$X^{(i)} := \begin{bmatrix} x_i^{(i)} \\ \{x_j^{(i)}\}_{j\in\mathcal{N}(i)} \end{bmatrix}$$

With this procedure, for $\rho > 0$, let the augmented Lagrangian be defined as

$$\begin{aligned}
&\mathcal{L}(X, Z, \Lambda, \mathcal{M}) \\
&= \sum_{i=1}^{N} \Bigg\{ p_i(X^{(i)}) \\
&\quad + \sum_{j\in\mathcal{N}(i)} \Big[\lambda_i^{(i,j)}\big(x_i^{(i)} - z_i^{(i,j)}\big) + \lambda_j^{(i,j)}\big(x_j^{(j)} - z_j^{(i,j)}\big)\Big] \\
&\quad + \sum_{j\in\mathcal{N}(i)} \Big[\mu_i^{(i,j)}\big(x_i^{(i)} - z_i^{(j,i)}\big) + \mu_j^{(i,j)}\big(x_j^{(i)} - z_j^{(j,i)}\big)\Big] \\
&\quad + \frac{\rho}{2} \sum_{j\in\mathcal{N}(i)} \Big[\|x_i^{(i)} - z_i^{(i,j)}\|^2 + \|x_j^{(i)} - z_j^{(i,j)}\|^2 \\
&\quad + \|x_i^{(i)} - z_i^{(j,i)}\|^2 + \|x_j^{(i)} - z_j^{(j,i)}\|^2 \Big] \Bigg\}
\end{aligned} \tag{7.7}$$

where every Lagrangian multiplier is a row vector with dimension 1×2 and the augmented Lagrangian is function only of the following three vectors containing local information, in addition to $X^{(i)}$:

$$Z^{(i)} := \begin{bmatrix} \{z_i^{(i,j)}\}_{j\in\mathcal{N}(i)} \\ \{z_j^{(i,j)}\}_{j\in\mathcal{N}(i)} \end{bmatrix}$$

$$\Lambda^{(i)} := \begin{bmatrix} \{\lambda_i^{(i,j)}\}_{j\in\mathcal{N}(i)} & \{\lambda_j^{(i,j)}\}_{j\in\mathcal{N}(i)} \end{bmatrix}$$

$$\mathcal{M}^{(i)} := \begin{bmatrix} \{\mu_i^{(i,j)}\}_{j\in\mathcal{N}(i)} & \{\mu_j^{(i,j)}\}_{j\in\mathcal{N}(i)} \end{bmatrix}$$

In this sense, node i stores in memory and updates few local variables.

Finally, let $Z^{(j_i)} := \{z_i^{(j,i)}, z_j^{(j,i)} | j \in \mathcal{N}(i)\}$ be the set containing all the edge variables referred to node i but stored (and updated) by its neighbours.

By denoting with t the iteration index, and considering the augmented Lagrangian (7.7), we have that at every iteration the following three steps are performed, in order:

1. Update of $X^{(i)},\ \forall i \in \mathcal{V}$:

$$X^{(i)}(t+1) = \underset{X^{(i)} \in \mathcal{C}_i}{\operatorname{argmin}}\ \mathcal{L}(X^{(i)}, Z^{(i)}(t), Z^{(j_i)}(t), \Lambda^{(i)}(t), \mathcal{M}^{(i)}(t)) \tag{7.8}$$

   This operation requires some effort and will be described in the next subsection.

2. Update of $Z^{(i)},\ \forall i \in \mathcal{V}$:

$$Z^{(i)}(t+1) = \underset{Z^{(i)}}{\operatorname{argmin}}\ \mathcal{L}(X^{(i)}(t+1), Z^{(i)}, Z^{(j_i)}(t), \Lambda^{(i)}(t), \mathcal{M}^{(i)}(t)) \tag{7.9}$$

   In this case, the closed form is easily obtainable by exploiting the component-wise gradient of (7.7) with respect to $z_k^{(i,j)}, k \in \{i, j\}$:

$$\frac{\partial \mathcal{L}}{\partial z_k^{(i,j)}} = -\lambda_k^{(i,j)\top}(t) - \mu_k^{(j,i)\top}(t) - \rho\big(x_k^{(i)}(t+1) + x_k^{(j)}(t+1)\big) + 2\rho z_k^{(i,j)}$$

   and by imposing it to be equal to zero, obtaining:

$$z_k^{(i,j)}(t+1) = \frac{\lambda_k^{(i,j)\top}(t) + \mu_k^{(j,i)\top}(t)}{2\rho} + \frac{x_k^{(i)}(t+1) + x_k^{(j)}(t+1)}{2} \tag{7.10}$$

3. Dual ascent step on $\Lambda^{(i)}$ and $\mathcal{M}^{(i)},\ \forall i \in \mathcal{V}$.

   $\Lambda^{(i)}$ and $\mathcal{M}^{(i)}$ are updated through a gradient ascent of $\mathcal{L}$ with step size ρ; namely, for $k \in \{i, j\}$:

$$\begin{aligned} \lambda_k^{(i,j)\top}(t+1) &= \lambda_k^{(i,j)\top}(t) + \rho\big(x_k^{(i)}(t+1) - z_k^{(i,j)}(t+1)\big) \\ \mu_k^{(i,j)\top}(t+1) &= \mu_k^{(i,j)\top}(t) + \rho\big(x_k^{(i)}(t+1) - z_k^{(j,i)}(t+1)\big) \end{aligned} \tag{7.11}$$

Notice that ρ, also called *penalty parameter*, is used as the step size α in the dual ascent method and is selected for good convergence speed. The convergence of this algorithm to the optimal point is ensured by the following

Proposition 4. *The sequence generated by the algorithm of equations (7.8), (7.9) and (7.11) converges to the optimal solution of the problem (7.6).*

Proof. The proof is well explained in [17] and is based on the fact that our approximated cost function is convex, the optimal solution set of problem (7.6) is nonempty and the intersection of the various $\mathcal{C}_i$ (i.e., the set of X satisfying (7.4b) and (7.4c)) is bounded. □

We now explain how the update of $X^{(i)}$ takes place, first introducing a couple of useful lemmas.

7.1 Update of $X^{(i)}$

Lemma 4. *If* $\lambda_k^{(i,j)}(0) = -\mu_k^{(j,i)}(0)$, $k \in \{i,j\}$, *then* $\lambda_k^{(i,j)}(t) = -\mu_k^{(j,i)}(t)$, $\forall t > 0$.

Proof. It can be proved by induction. Let $\lambda_k^{(i,j)}(l) = \mu_k^{(j,i)}(l)$, for $l = 0, \dots, t-1$. Then the updates take the form:

$$\begin{aligned}
\lambda_k^{(i,j)\top}(t) &= \lambda_k^{(i,j)\top}(t-1) + \rho\big(x_k^{(i)}(t) - z_k^{(i,j)}(t)\big) \\
&\overset{(a)}{=} \lambda_k^{(i,j)\top}(t-1) + \rho\bigg(x_k^{(i)}(t) - \frac{\lambda_k^{(i,j)\top}(t-1) + \mu_k^{(j,i)\top}(t-1)}{2\rho} \\
&\qquad - \frac{x_k^{(i)}(t) + x_k^{(j)}(t)}{2}\bigg) \\
&\overset{(b)}{=} \lambda_k^{(i,j)\top}(t-1) + \rho\frac{x_k^{(i)}(t) - x_k^{(j)}(t)}{2}
\end{aligned}$$

where in (a) equations (7.10) have been used and equivalence (b) comes from the inductive hypothesis. In a similar way we obtain

$$\mu_k^{(j,i)\top}(t) = \mu_k^{(j,i)\top}(t-1) + \rho\frac{x_k^{(j)}(t) - x_k^{(i)}(t)}{2}$$

from which, by the inductive hypothesis, it can be noticed that $\lambda_k^{(i,j)}(t) = -\mu_k^{(j,i)}(t)$. □

Lemma 5. *If* $\lambda_k^{(i,j)}(0) = -\mu_k^{(j,i)}(0)$, $k \in \{i,j\}$, *then* $z_k^{(i,j)}(t) = z_k^{(j,i)}(t)$, $\forall t > 0$.

Proof. From (7.10) and Lemma 4, we have

$$\begin{aligned}
z_k^{(i,j)}(t) &= \frac{\lambda_k^{(i,j)\top}(t-1) + \mu_k^{(j,i)\top}(t-1)}{2\rho} + \frac{x_k^{(i)}(t) + x_k^{(j)}(t)}{2} \\
&= \frac{x_k^{(i)}(t) + x_k^{(j)}(t)}{2} = z_k^{(j,i)}(t)
\end{aligned}$$

□

Lemma 6. *If* $\lambda_k^{(i,j)}(0) = \mu_k^{(i,j)}(0)$, $k \in \{i,j\}$, *then* $\lambda_k^{(i,j)}(t) = \mu_k^{(i,j)}(t)$, $\forall t > 0$.

Proof. Let $\lambda_k^{(i,j)}(l) = \mu_k^{(i,j)}(l)$, $l = 0, \dots, t-1$. Then

$$\begin{aligned}
\lambda_k^{(i,j)\top}(t) = \lambda_k^{(i,j)\top}(t-1) + \rho\bigg(x_k^{(i)}(t) - \frac{\lambda_k^{(i,j)\top}(t-1) + \mu_k^{(j,i)\top}(t-1)}{2\rho} \\
- \frac{x_k^{(i)}(t) + x_k^{(j)}(t)}{2}\bigg)
\end{aligned} \tag{7.12}$$

and

$$\mu_k^{(i,j)\top}(t) = \mu_k^{(i,j)\top}(t-1) + \rho\Bigg(x_k^{(i)}(t) - \frac{\lambda_k^{(j,i)\top}(t-1) + \mu_k^{(i,j)\top}(t-1)}{2\rho} - \frac{x_k^{(j)}(t) + x_k^{(i)}(t)}{2}\Bigg) \tag{7.13}$$

The subtraction (7.12)-(7.13) gives

$$\begin{aligned}
&\lambda_k^{(i,j)\top}(t) - \mu_k^{(i,j)\top}(t) \\
&= \cancel{\lambda_k^{(i,j)\top}}(t-1) - \cancel{\mu_k^{(i,j)\top}}(t-1) + \frac{1}{2}\big(-\cancel{\lambda_k^{(i,j)\top}}(t-1) - \cancel{\mu_k^{(j,i)\top}}(t-1) \\
&\quad + \cancel{\lambda_k^{(j,i)\top}}(t-1) + \cancel{\mu_k^{(i,j)\top}}(t-1)\big)
\end{aligned}$$

where simplifications are allowed by the inductive hypothesis. Therefore, $\lambda_k^{(i,j)\top}(t) = \mu_k^{(i,j)\top}(t)$. □

At this point we can state a simple but useful

Corollary 1. *If $\lambda^{(i,j)} = -\mu^{(j,i)} = \mu^{(i,j)} = -\lambda^{(j,i)}$, then:*

- $z_k^{(i,j)}(t+1) = z_k^{(j,i)}(t+1) = \dfrac{x_k^{(i)}(t+1) + x_k^{(j)}(t+1)}{2},\ k \in \{i,j\}$
- $\lambda_k^{(i,j)\top}(t+1) = \lambda_k^{(i,j)\top}(t) + \dfrac{\rho}{2}(x_k^{(i)}(t+1) - x_k^{(j)}(t+1)),\ k \in \{i,j\}$

These three lemmas allow to simplify the expression for $\mathcal{L}$ (7.7) in the following way:

$$\begin{aligned}
\mathcal{L}(X,Z,\Lambda) = \sum_{i=1}^{N}\Bigg\{ & p_i(X^{(i)}) \\
& + \sum_{j\in\mathcal{N}(i)}\Big[2\lambda_i^{(i,j)}\big(x_i^{(i)} - z_i^{(i,j)}\big) + 2\lambda_j^{(i,j)}\big(x_j^{(i)} - z_j^{(i,j)}\big)\Big] \\
& + \rho\sum_{j\in\mathcal{N}(i)}\Big[\|x_i^{(i)} - z_i^{(i,j)}\|^2 + \|x_j^{(i)} - z_j^{(i,j)}\|^2\Big]\Bigg\}
\end{aligned} \tag{7.14}$$

We can then focus our attention on those parts of (7.14) which are effectively dependent on $X^{(i)}$. In other words, minimizer (7.8) can be replaced by

$$X^{(i)}(t+1) = \underset{X^{(i)}\in\mathcal{C}_i}{\operatorname{argmin}}\ \mathcal{L}^i(X^{(i)}, Z^{(i)}(t), \Lambda^{(i)}(t)) \tag{7.15}$$

where

$$\begin{aligned}
&\mathcal{L}^i(X^{(i)}, Z^{(i)}(t), \Lambda^{(i)}(t)) = \\
&= p_i(X^{(i)}) + X^{(i)\top}M_iX^{(i)} - X^{(i)\top}B^{(i)}(t)
\end{aligned} \tag{7.16}$$

with

$$M_i := \rho \begin{bmatrix} |\mathcal{N}(i)| I_2 & 0 \\ 0 & I \end{bmatrix}$$

$$F^{(i)}(t) := \begin{bmatrix} \sum_{j \in \mathcal{N}(i)} \lambda_i^{(i,j)}(t) & \{\lambda_j^{(i,j)}(t)\}_{j \in \mathcal{N}(i)} \end{bmatrix}$$

$$G^{(i)}(t) := \rho \begin{bmatrix} \sum_{j \in \mathcal{N}(i)} x_i^{(j)}(t) - x_i^{(i)}(t) \\ \{x_j^{(j)}(t) - x_j^{(i)}(t)\}_{j \in \mathcal{N}(i)} \end{bmatrix}$$

$$B^{(i)}(t) := 2M_i X^{(i)}(t) + G^{(i)}(t) - 2F^{(i)\top}(t)$$

For the calculations, see Appendix B.

Therefore, minimizer (7.15), which is equivalent to minimizer (7.8), has the simpler expression

$$X^{(i)}(t+1) = \underset{X^{(i)} \in \mathcal{C}_i}{\operatorname{argmin}} \; p_i(X^{(i)}) + X^{(i)\top} M_i X^{(i)} - X^{(i)\top} B^{(i)}(t) \tag{7.17}$$

Minimizer (7.17) can be efficiently calculated by many tools, without the need of calculating a closed form for it.

We can finally summarize our ADMM-based algorithm.

7.2 ADMM-based algorithm

Let θ be the impedance angle defined in assumption 2 in subsection 3.1.2, and $\mathcal{C}_i$ be the feasible set of local voltages, where the physical bounds $\underline{p}_i$, $\overline{p}_i$, $\underline{q}_i$, $\overline{q}_i$ are verified. Let ρ be the step size parameter a priori assigned and Y the real-valued Laplacian of the grid model. At every synchronous iteration, each node i except the PCC executes the following ordered operations:

1. transmission of $X^{(i)}$ and reception of $X^{(j)}$ to and from its neighbours j;
2. $$G^{(i)} \leftarrow \rho \begin{bmatrix} \sum_{j \in \mathcal{N}(i)} x_i^{(j)} - x_i^{(i)} \\ \{x_j^{(j)} - x_j^{(i)}\}_{j \in \mathcal{N}(i)} \end{bmatrix}$$
3. $$F^{(i)} \leftarrow F^{(i)} - \frac{G^{(i)\top}}{2}$$
4. $$B^{(i)} \leftarrow 2M_i X^{(i)} + G^{(i)} - 2F^{(i)\top}$$
5. $$X^{(i)} \leftarrow \underset{X^{(i)} \in \mathcal{C}_i}{\operatorname{argmin}} \; p_i(X^{(i)}) + X^{(i)\top} M_i X^{(i)} - X^{(i)\top} B^{(i)}$$

8

Simulations and results

In this chapter we propose some specific simulations in order to validate the algorithms described in the previous chapters. To do that, we run our methods over the IEEE37 Test Feeder [10], whose graph structure is shown in Figure 8.1, using MATLAB®.

In all the simulations we make use of MATPOWER, a package of MATLAB M-files for solving power flow and optimal power flow [9]. It represents an efficient and recognized tool, so in this context it is used to simulate the application on the effective grid of the electrical quantities computed with our algorithms and to make meaningful comparisons between, for example, the optimal value we obtain with the global optimal one. The initial high values of the power losses is due to the fact that all the distributed generators are off at the beginning, and all the required powers are provided by the PCC.

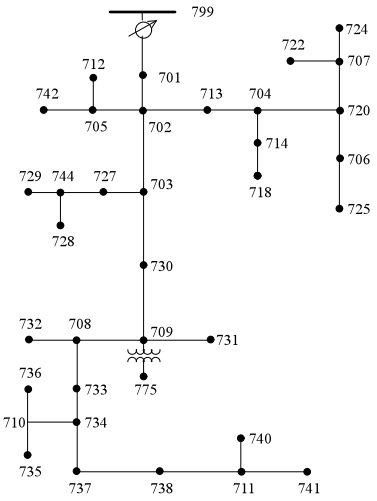

Figure 8.1: IEEE37 test feeder graph.

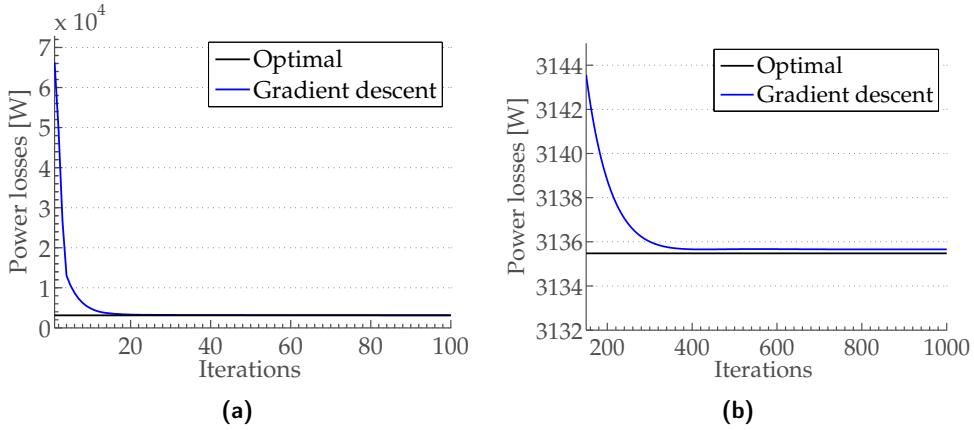

Figure 8.2: Comparison of optimal losses and losses resulting from the Gradient Projection algorithm: subfigure 8.2a shows only the first 100 iterations for a better visualization of the (brief) transient, while 8.2b shows the steady state behaviour.

8.1 Results of the Gradient Projection approach

We first discuss the power losses evolution for the Gradient Projection algorithm discussed in Chapter 5.

We recall that the calculations involve an approximated model of the grid (one approximation, for example, is represented by the assumption that all the power lines has the same inductance/resistance ratio θ), while the application takes place, through MATPOWER, to a different one.

As Figure 8.2 suggests, this imperfect knowledge does not cause evident problems to the Gradient Projection algorithm: at every iteration probably it does not follow the exact gradient direction, but a direction which is not so far from it (in some sense, a subgradient), being able to reach a point very close to the optimal one (see subfigure 8.2b for the steady state).

8.2 Results of the Dual Ascent approach

8.2.1 Only generators as agents

In this section, we discuss the results obtained for the Dual Ascent approach when only generators (in this case 7 of 36 nodes, including the PCC) are considered as smart agents, i.e. have sensing and computational capabilities. We have seen that the updates of the primal variables (Equation (6.5) and (6.6)) are dependent on some unmonitored quantities represented by the load active and reactive power demands. Then, it has been demonstrated how they can be estimated starting from the knowledge of the topology and voltage

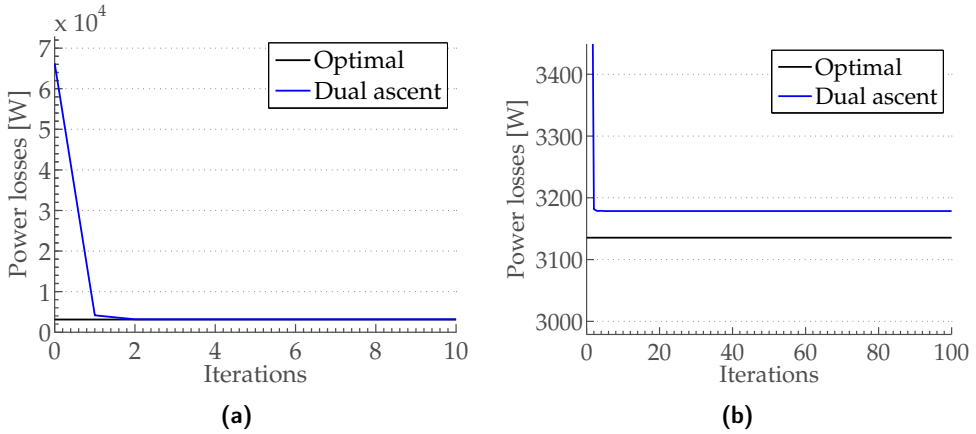

Figure 8.3: Comparison between optimal losses and losses resulting from the dual ascent-based algorithm with feedback strategy for the estimation of the load demand: subfigure 8.3a shows only the first 10 iteration for a better visualization of the (brief) transient, while 8.3b shows how the algorithm goes near to the optimal value, but without reaching it.

measurements of the generators, ending with the local formulations (6.13) and (6.14). The dual variables, instead, does not have this kind of problem, being dependent on monitored (in other words, decisional) variables.

Figure 8.3 describes how this algorithm works: we have a very fast convergence to a point which is not exactly the optimal one, but is very close to it.

8.2.2 Both generators and loads as agents

We now discuss the results of the Dual Ascent approach to the second case, where all the nodes of the grid are able to update and communicate the Lagrange multipliers. In this scenario the updates of the primal variables were only functions of the Lagrange multipliers of the neighbours, as summarized in the expressions (6.31) and (6.32). Furthermore, also the evolution of the dual variables is dependent only on the decisional variables, as before.

Figure 8.4 shows the performance of this algorithm: the number of iterations needed for a substantial convergence is higher than before, and this can be explained if we consider the higher number of Lagrange multipliers that has to be updated and exchanged. On the contrary, the whole cycle takes place without applying anything to the grid, and this allows to not have some problems which could arise in the previous approach and concerning the cost of the iterative application of power to the grid and the time needed for the a correct estimation of the unmonitored nodes.

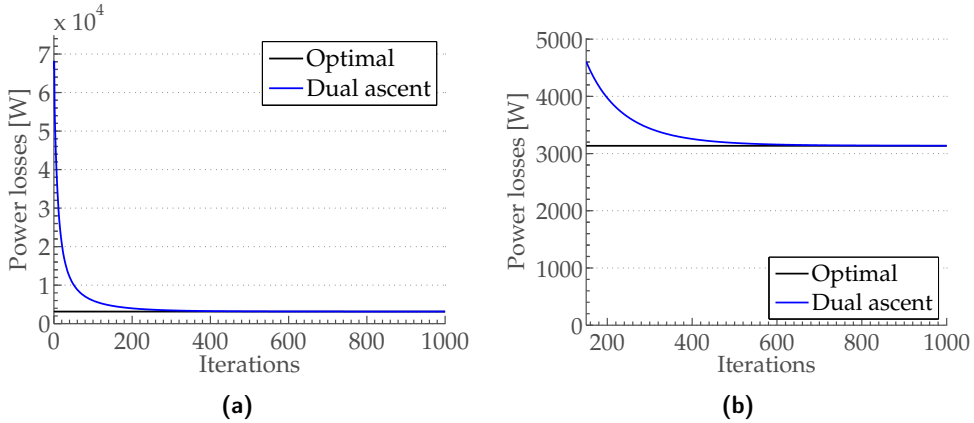

Figure 8.4: Comparison between optimal losses and losses resulting from the dual ascent-based algorithm when no actuations and measures take place during the cycle: subfigure 8.4b represents the zoom on the last iterations of 8.4a.

8.3 Results of the ADMM-based approach

In this section we study the behaviour of the ADMM-based algorithm. By recalling that in this context for a certain physical quantity x the notation $x_j^{(i)}$ means the value calculated by node i and referring to node j, we have that at steady state the solution to the OPF problem, for each node k, is given by $u_k = u_k^{(k)}$ [16]. Figure 8.5 shows the power losses that we would have at every iteration if the specific voltages (uniquely corresponding to specific power injections) are applied.

We can notice that the algorithm is able to reach the optimal value (the plot in 8.5b is still decreasing), even if it requires a number of iterations quite high.

In addition to the power losses, it is interesting to analyse the convergence of various quantities of the distributed ADMM-based algorithm. This is due to the particular formulation of the resolution procedure, in which at every iteration each node computes the optimal voltages for itself and its neighbours in order to minimize its own power injection. Step by step the algorithm reduces the initial divergence of "opinion" of the different nodes, allowing to reach at the end a point which results feasible.

Plots in Figure 8.6 give an exhaustive vision about how algorithm works.

Figure 8.6a shows the convergence of the voltages vector to a specific (we can state optimal, given Figure 8.5) vector. In fact, for each iteration t the following quantity has been calculated and plotted:

$$\|u(t) - u(t-1)\| = \sum_{i \in \mathcal{V}} \sqrt{(u_i^{(i)}(t) - u_i^{(i)}(t-1))^2}$$

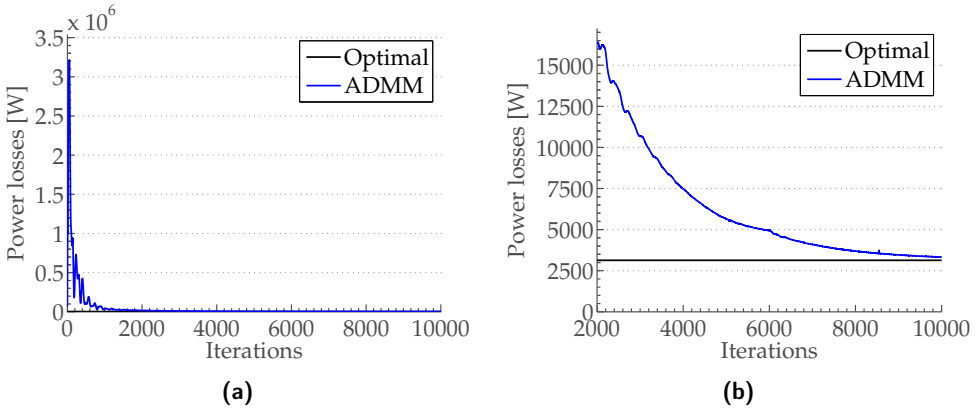

Figure 8.5: Comparison between optimal losses and losses resulting from the ADMM-based algorithm: subfigure 8.5b represents the zoom on the last iterations of 8.5a.

The resulting plot shows how this quantity tends to zero for large values of the iteration index, confirming what we could deduce from the convergence of the losses plot. Another aspect that is important to be monitored is the convergence of the opinion of the nodes about the nodal voltages. By recalling that a node i computes the voltage that node j should have only if $j \in \mathcal{N}(i) \cup \{i\}$, and by denoting with $\mu_{i_{\text{Re}}}$ and $\mu_{i_{\text{Im}}}$ the following average values:

$$\mu_{i_{\text{Re}}} = \frac{1}{|\mathcal{N}(i)|+1} \sum_{j \in \mathcal{N}(i) \cup \{i\}} u_{i_{\text{Re}}}^{(j)} \quad , \quad \mu_{i_{\text{Im}}} = \frac{1}{|N(i)|+1} \sum_{j \in \mathcal{N}(i) \cup \{i\}} u_{i_{\text{Im}}}^{(j)}$$

we have that Figure 8.6b well describes this problem, since it represents the function:

$$\frac{1}{|\mathcal{V}|} \sum_{i \in \mathcal{V}} \left[\frac{1}{|\mathcal{N}(i)|+1} \sum_{j \in \mathcal{N}(i) \cup \{i\}} \left[(u_{i_{\text{Re}}}^{(j)}(t) - \mu_{i_{\text{Re}}}(t))^2 + (u_{i_{\text{Im}}}^{(j)}(t) - \mu_{i_{\text{Im}}}(t))^2 \right] \right]$$

that is the average (on all nodes $i \in \mathcal{V}$) of the variance of the voltages referring to node i computed by i itself and its neighbours. The convergence of this last quantity is fundamental for the feasibility of the calculated set of voltages. In fact, the feasibility for a certain node i would be assured at every iteration if the voltages of node i and its neighbours computed by node i itself were applied. But as we have seen, the voltages we consider are constituted by $u_i^{(i)}$. The feasibility of the whole vector of voltages is then reached when the difference of opinion is neglectable, i.e. when the variance (just shown in Figure 8.6b) tends to zero. This intuition is confirmed by Figure 8.6c, that represents how much far we are from the required ranges of power injection for generators and power demands for loads; in fact, the following function depending on the

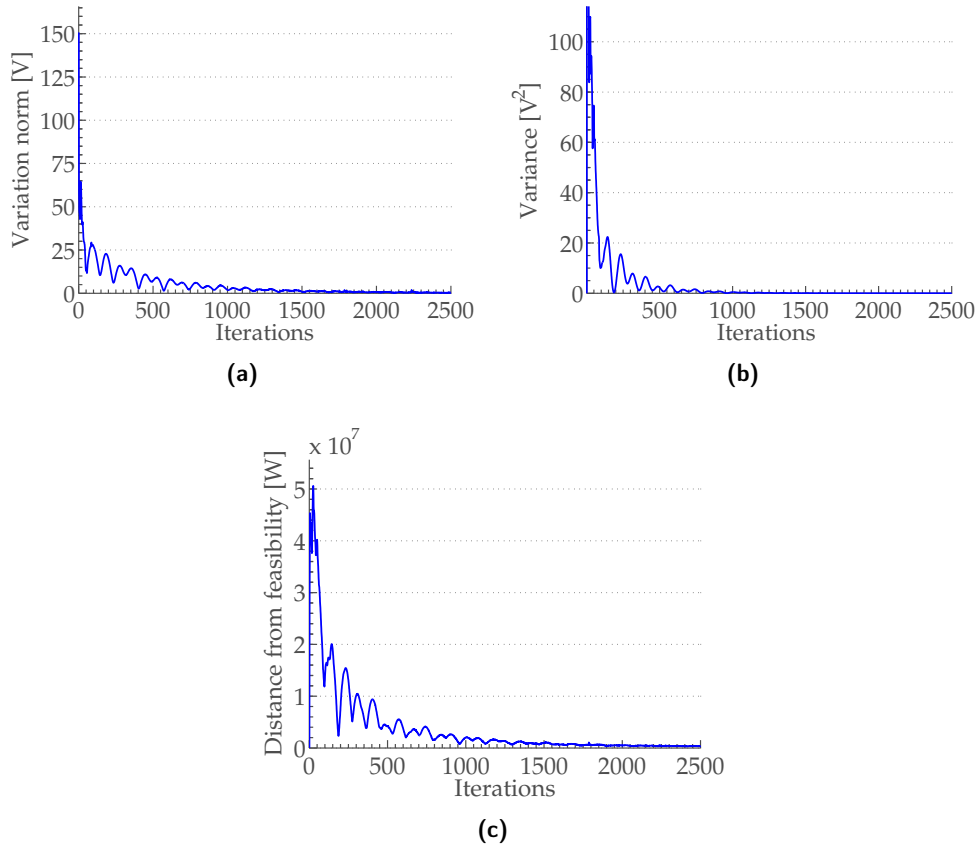

Figure 8.6: Plot of some interesting quantities for evaluating the convergence of the ADMM-based algorithm: 8.6a is the norm of the difference of two consecutive nodal voltage vectors, 8.6b shows the variance concerning the nodal "opinions" on the different voltages, 8.6c shows the distance of the solution achieved to the given bounds.

iteration index t has been plotted:

$$\begin{aligned} y(t) = &\sum_{i\in\mathcal{L}} |p(t)_i - \overline{p}_i| + |q(t)_i - \overline{q}_i| \\ &+ \sum_{i\in\mathcal{C}} \Big[[p(t)_i - \overline{p}_i]\mathbb{1}(p(t)_i - \overline{p}_i) + [\underline{p}_i - p(t)_i]\mathbb{1}(\underline{p}_i - p(t)_i) \\ &\quad + [q(t)_i - \overline{q}_i]\mathbb{1}(q(t)_i - \overline{q}_i) + [\underline{q}_i - q(t)_i]\mathbb{1}(\underline{q}_i - q(t)_i) \Big] \end{aligned} \tag{8.1}$$

where we have introduced the function

$$\mathbb{1}(x) = \begin{cases} 1 & \text{if } x \geq 0 \\ 0 & \text{otherwise} \end{cases}$$

and where we recall that $\overline{p}_i = \underline{p}_i$ and $\overline{q}_i = \underline{q}_i$, $\forall i \in \mathcal{L}$.

8.4 Final results

We can finally collect all the results of the algorithms, obtaining Table 8.1. The following values are shown:

- iterations$_{<10\%}$: the required number of iterations in order to have power losses exceeding the optimal ones less than 10% - it gives an idea of the fastness of the algorithm to reach an acceptable value;
- steady state value: the steady state value of the power losses - in some sense, it exploits the precision of the algorithms in reaching the optimal point;
- steady state gap: it represents the difference of the reached value and the optimal one (percentage);
- smart agents: the number of agents which is assumed for a specific algorithm;
- actuations: the total number of actuations occurring in the grid at every iteration;
- measurements: the total number of measurements occurring in the grid at every iteration;
- communications: the total number of communication activities (neglecting the effective amount of data) at every iteration.

Table 8.1: Collection of some of the most interesting results and features obtained in the previous sections.

	Grad. Proj.	Dual Ascent $\mathcal{A} \equiv \mathcal{C}$	Dual Ascent $\mathcal{A} \equiv \mathcal{V}$	ADMM
iterations$_{<10\%}$ [#]	17	2	298	9064
s.s. value [W]	3135.7	3178.5	3135.8	3135.5
s.s. gap [%]	0.0064	1.3713	0.011	0
smart agents [#]	7	7	36	36
actuations [#]	7	7	0	0
measurements [#]	7	7	0	0
communications [#]	16	16	69	70

8.5 Robustness

8.5.1 Robustness with respect to grid parameters

In this section we study the performance of the algorithms described so far when the estimated grid differs from the original one, in particular for what concerns the line impedances.

It means that we run our algorithms on a certain model represented by the vector of impedances z_{err}, with consequent determination of matrices Z, Y, X and so on, while the model on which we apply the calculated power injections, measure the nodal voltages and calculate the effective power losses is represented by z_{true}.

We now discuss some interesting results for a great number of particular realizations of the error, which is assumed to have a uniform distribution (with mean corresponding to the true value); the results shown in Figure 8.7 and 8.8 are referred to maximum errors of the $\pm 10\%$ and $\pm 30\%$ on the true value, respectively.

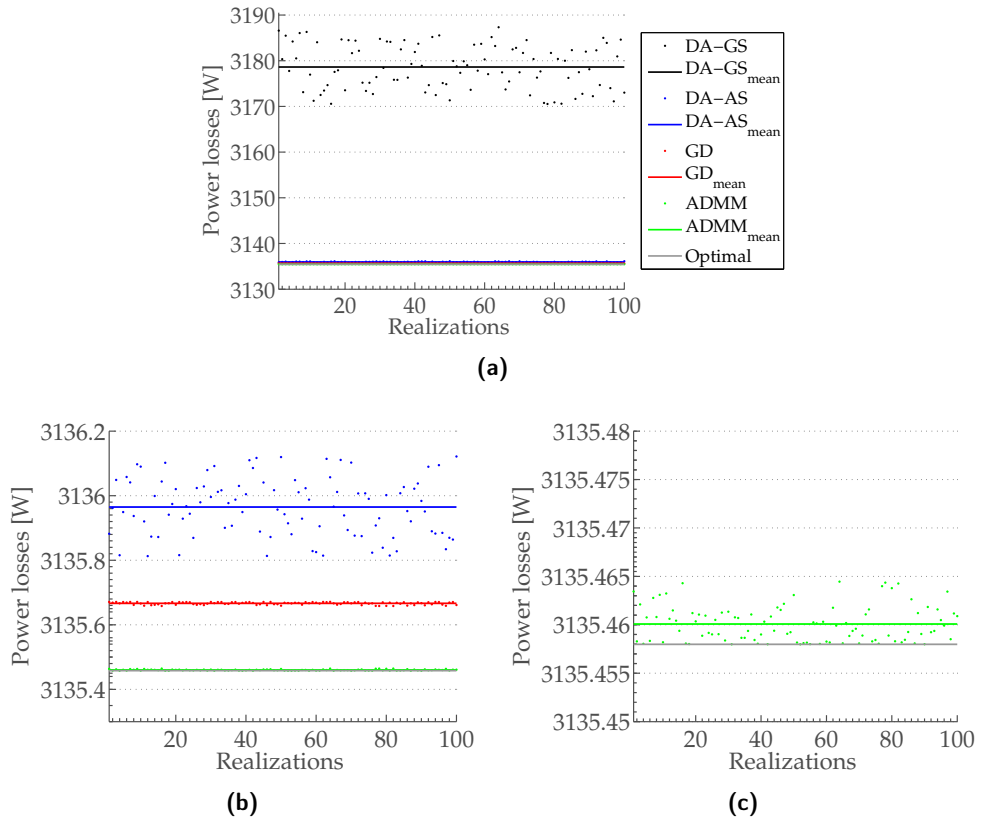

Figure 8.7: Comparison of the robustness of the algorithms for 100 realizations with maximum error of the $\pm 10\%$. Subfigures 8.7b and 8.7c represent the zoom, on different levels, of 8.7a.

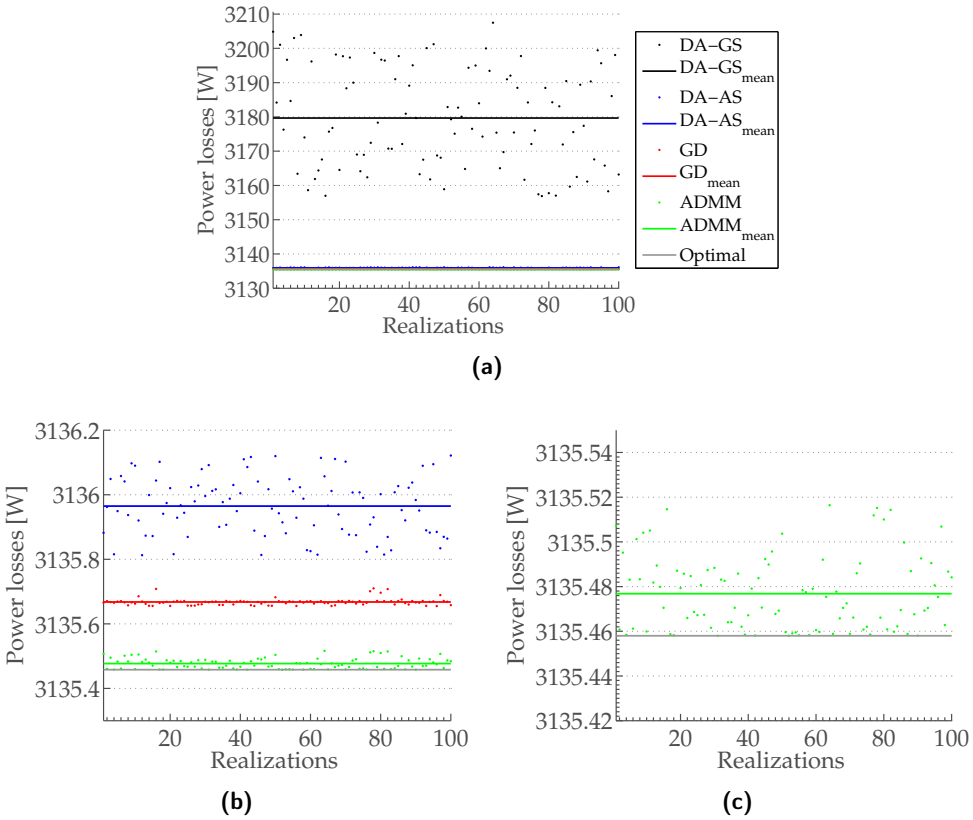

Figure 8.8: Comparison of the robustness of the algorithms for 100 realizations with maximum error of the ±30%. Subfigures 8.8b and 8.8c represent the zoom, on different levels, of 8.8a.

In these figures several data are plotted, and the abbreviations used in the legends are GD (Gradient Descent, referring to the gradient projection approach), DA (Dual Ascent), ADMM (obviously, Alternating Direction Multiplier Method), GS (only Generators as Smart agents) and AS (All nodes as Smart agents).

We can see that for every realization we obtain a different optimal value, but the dispersion is not so large and, most important, the mean value is very close, for every algorithm, to the optimal obtained with the approximated, but without further errors, model.

This fact can be justified if we consider that every algorithm tries to minimize the power losses and this happens if, roughly speaking, the power demand of a certain load is provided by those generators that are the nearest to it, with a light dependence on the (effective or estimated) line impedances. The reasoning is that in some sense the topology covers a much more important role respect to the precise knowledge of the line impedances.

It is then interesting to notice that for dual ascent algorithm the perfor-

mance when only generators are smart agents are worse than the performance when all nodes are smart agents. This is explainable if we consider that in the first case there is a deeper dependence on the grid parameters, because they are used also for the estimation of the power demands: a wrong knowledge of the power demand implies a worse distributed injection, with consequences on the total power losses.

8.5.2 Robustness with respect to grid topology

Our study of the robustness of the algorithms continues by analysing their behaviour when errors related to the grid topology occur. It means that the algorithms make use of a certain model which is different from the actual grid for what concerns the location of some nodes. This can be simulated by changing some elements of the adjacency matrix A, more precisely by randomly changing the position of the external nodes, that are the nodes that have only one (electric) neighbour: the reason behind this choice is to avoid the random creation of electric rings or the birth of two or more disconnected graphs.

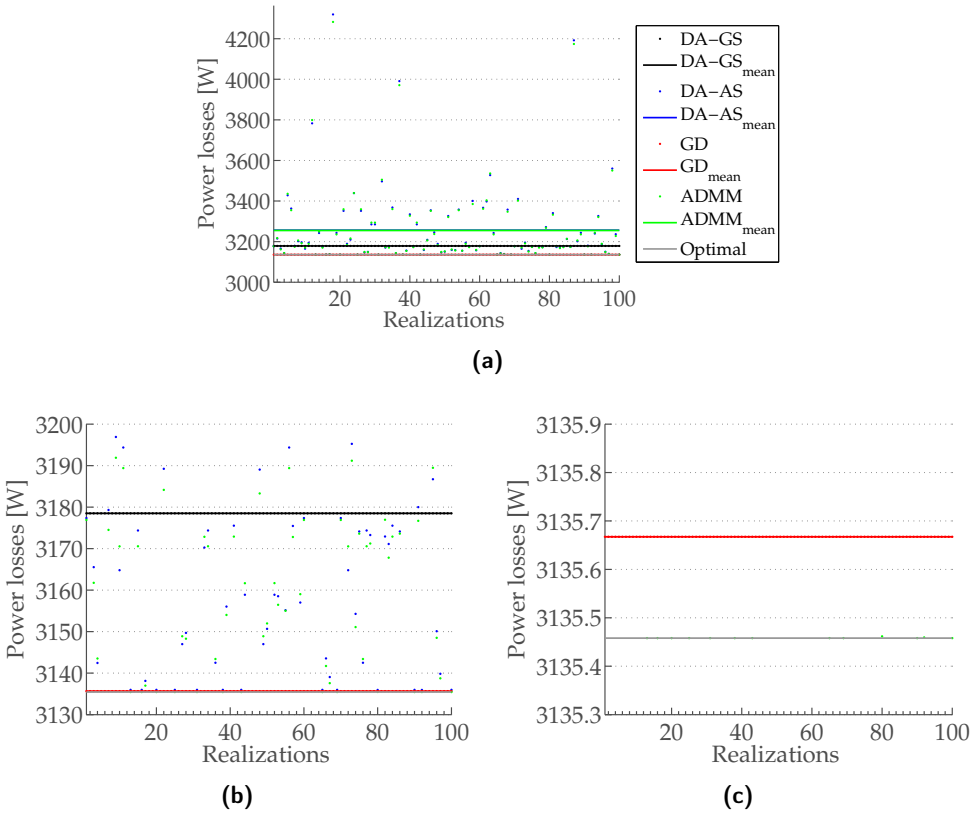

Figure 8.9: Comparison of the robustness of the algorithms for 100 realizations with a load in a wrong position. Subfigures 8.9b and 8.9c represent the zoom, on different levels, of 8.9a.

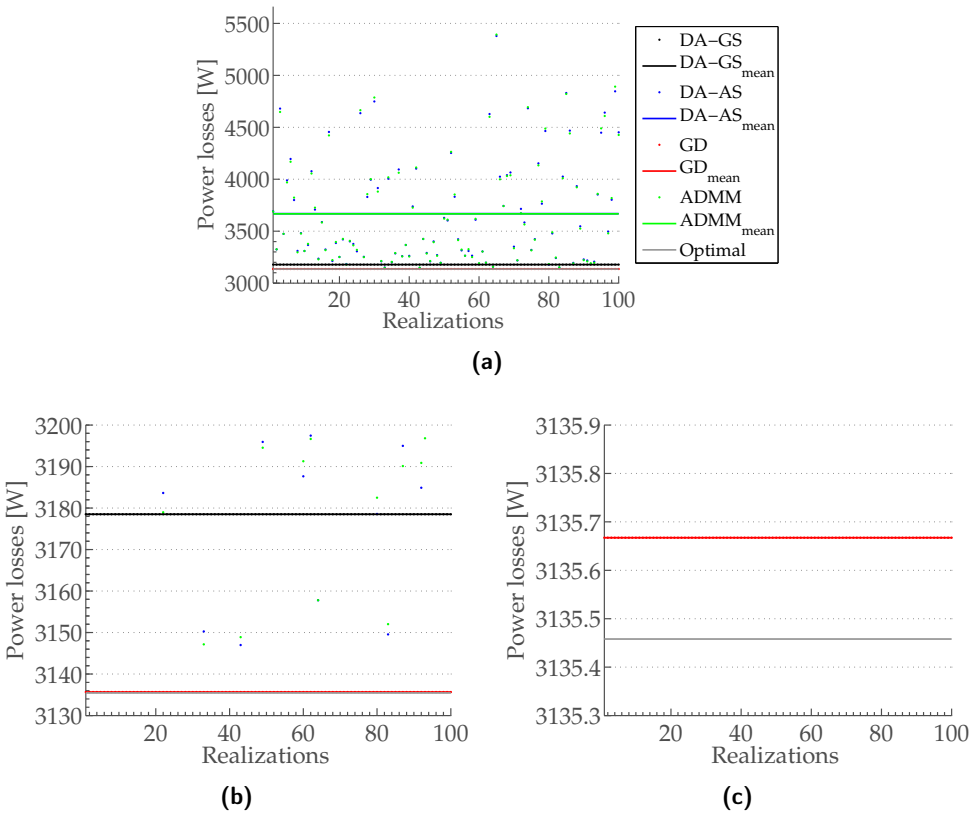

Figure 8.10: Comparison of the robustness of the algorithms for 100 realizations with 3 loads in a wrong position. Subfigures 8.10b and 8.10c represent the zoom, on different levels, of 8.10a.

Figure 8.9 shows the performance of the algorithms when only a node is positioned in a different place, while Figure 8.10 refers to the case in which three loads have wrong positions.

It is interesting to notice how the Gradient Projection and the Dual Ascent - only generators as agents - algorithms are not influenced by this kind of error, because they estimate the power demands of the loads by directly measuring the nodal voltages obtained by the application of the power injections of the previous instant; in this situation the feedback control strategy avoids any kind of error. On the contrary, the algorithms characterized by a unique final actuation are strongly dependent on the correctness of the model, and provide a set of power injections that is quite far from the optimal one.

In the end, some specific realizations reserve to be further studied. Consider the realization number 20. As subfigures 8.9b and 8.9c show, also the Dual Ascent - all nodes as agents - and the ADMM algorithms are very close to the optimal value, apparently in disagreement with what has just been said. In reality, in this case it has been verified that the node with label 724 (see Figure 8.1) has been randomly connected to the node with label 707, then obtaining

the original grid! Even more interesting is the realization number 80, where the reached value is slightly above the optimal. In this case the node with label 735 results connected to the number 734, giving birth to a grid that is different but not so much from the original one.

As said, Figure 8.10 shows the random placement of three loads, with the consequent greater dispersion and worsening of the performance of those algorithms which does not make use of the nodal voltage measurements. In this case, the lucky eventuality to obtain a configuration almost identical to the original one has very low probability, as confirmed by the always high value of these algorithms.

In the end, the average value for the Dual Ascent - all nodes as agents - is very close to the ADMM mean value (this is the reason why it seems to be absent), as proven by the very close values reached for every realization.

8.5.3 Final results for robustness

We finally propose the numerical results regarding the robustness of the different approaches with respect to the kinds of error we have just discussed.

Table 8.2 summarizes the following quantities:

- variance: it refers to the dispersion of the values obtained for every specific realization of the errors, and represents the quantity

$$\frac{1}{N}\sum_{i=1}^{N}(x_i-\mu)^2$$

  where N is the number of realizations (in this case, $N = 100$), x_i is the value obtained with the i-th error configuration and μ is the average value of the x_i, $i = 1, \ldots, N$;

- steady state gap: similarly to that introduced in Table 8.1, it represents the difference of the mean value and the optimal one (percentage).

Each of the previous quantities has been calculated for all the different error scenarios we described so far:

- $\pm 10\%$: error regarding the line impedance values, and maximum (absolute) value of the 10% on the correct one and with uniform distribution;
- $\pm 30\%$: as before, but with support defined by the $\pm 30\%$ of the exact value;
- 1 (load): when a load is estimated in a wrong position;
- 3 (loads): as before, but with three bad estimated load locations.

Table 8.2: Collection of some of the most interesting results about the robustness of the algorithms with respect to different kinds of errors.

	Kind of error	Grad. Proj.	Dual Ascent $\mathcal{A} \equiv \mathcal{C}$	Dual Ascent $\mathcal{A} \equiv \mathcal{V}$	ADMM
variance [V^2]	±10%	$1.6 \cdot 10^{-5}$	22.9	$7.5 \cdot 10^{-3}$	$3.4 \cdot 10^{-6}$
	±30%	$1.13 \cdot 10^{-4}$	205.16	$1.02 \cdot 10^{-2}$	$2.73 \cdot 10^{-4}$
	1	0	0	$3.87 \cdot 10^{4}$	$3.75 \cdot 10^{4}$
	3	0	0	$2.565 \cdot 10^{5}$	$2.567 \cdot 10^{5}$
s.s. gap [%]	±10%	$6.6 \cdot 10^{-3}$	1.38	0.016	$6.7 \cdot 10^{-5}$
	±30%	$6.7 \cdot 10^{-3}$	1.41	0.017	$6.01 \cdot 10^{-4}$
	1	$6.7 \cdot 10^{-3}$	1.37	3.85	3.81
	3	$6.7 \cdot 10^{-3}$	1.37	17.01	16.95

9 Conclusions

The thesis formalizes the optimal power flow problem, by offering multiple formulations (each one more or less applicable, depending on the context) and different strategies of solution. In some sense, it collects and compares the approaches outlined by different lines of research: the first one proposes a grid with few smart agents, with a sort of feedback control law for estimating the unknown but necessary quantities and for keeping track, in some sense, of the grid state evolution; the second one assumes that every node has some sensing, communication and computing capabilities, and consists in a long part of communication and computation followed, only at the end, by the actuation.

Therefore, starting from these works, a specific and realistic scenario (with lower and upper bounds on the power injections) has been proposed and developed, obtaining a consistent vision and comparison of formulations at the beginning so different.

We can conclude that:

- the feedback control strategies have several advantages, because they
  - require a limited number of smart agents, that are constituted by the generators only,
  - converge to a value that can be considered almost optimal in few iterations,
  - have a good robustness with respect to a certain kind of topology errors,

  but have some limitations, such as
  - a continuous application and sensing activity, with probable higher costs,

  - the need of waiting the settling of the electrical quantities before performing meaningful measurements and starting the subsequent iteration,
  - higher sensitivity to line impedance errors;

- the other strategies, that are the second version of the dual ascent method and the ADMM, are characterized by

  - an unique final actuation, without any measurements (but only communications) from one iteration and the next one,
  - performance depending only on the computing and communication capabilities, regardless the grid dynamics,
  - lower sensitivity to line impedance errors,

  but, on the other hand,

  - typically require an high number of iterations, especially for what concerns the ADMM in the consensus form here discussed,
  - assume that all nodes have computation and communication capabilities,
  - are highly dependent on the correctness of the grid topology.

The results could be deeper studied in the future by considering, first of all, not only the number of iterations needed for each algorithm, but also the time required for the different computations and communications. Secondly, it could be interesting to understand if there is a cost or some kinds of issues in applying the power injections and measuring the nodal voltages at every iteration and, on the other hand, what is the cost (in terms of energy losses) of actuating only at the end of a (likely) quite long computation. In the end, a certain number of studies can be done concerning the ability of the different approaches to follow a dynamical load profile or in an asynchronous scenario.

A

Cost function derivation

In this appendix the formulas concerning the cost functions used in Chapter 5 are derived.

A.1 Cost function for Gradient Projection and Dual Ascent approaches

We now show where Equation (5.2) comes from.

Firstly, let us derive Equation (5.1), by expressing the power losses in terms of the node voltages:

$$\begin{aligned} J_{\text{losses}} &= \sum_{e\in\mathcal{E}} |\xi_e|^2 \operatorname{Re}\{z_e\} \\ &= \bar{\xi}^\top \operatorname{Re}\{\boldsymbol{Z}\}\xi \\ &= \bar{\xi}^\top Z\xi \cos\theta \\ &= (-e^{j\theta}\bar{u}^\top A^\top Z^{-1}) Z (-e^{-j\theta} Z^{-1} A u) \cos\theta \\ &= \bar{u}^\top A^\top Z^{-1} A u \cos\theta \\ &= \bar{u}^\top Y u \cos\theta \end{aligned} \tag{A.1}$$

From Proposition 2 in Chapter 5, we have

$$u \approx e^{j\varphi}\left(U_N \mathbf{1} + \frac{e^{j\theta}}{U_N}\begin{bmatrix} 0 & \mathbf{0} & \\ \mathbf{0} & M & N \\ \mathbf{0} & N^\top & O \end{bmatrix}\begin{bmatrix} 0 \\ \bar{s}_{\text{in}} \end{bmatrix}\right)$$

where the approximation consists in a term which is $o\left(\frac{1}{U_N}\right)$.

Then we can write:

$$
\begin{aligned}
\bar{u}^\top Y u &\approx e^{-j\varphi}\left(U_N\mathbf{1}^\top + \frac{e^{-j\theta}}{U_N}\begin{bmatrix}0 & s_G^\top & s_L^\top\end{bmatrix}X^\top\right)Ye^{j\varphi}\left(U_N\mathbf{1} + \frac{e^{j\theta}}{U_N}X\begin{bmatrix}0\\ \bar{s}_G\\ \bar{s}_L\end{bmatrix}\right)\\
&\overset{(a)}{=} \frac{1}{U_N^2}\begin{bmatrix}0 & s_G^\top & s_L^\top\end{bmatrix}XYX\begin{bmatrix}0\\ \bar{s}_G\\ \bar{s}_L\end{bmatrix}\\
&\overset{(b)}{=} \frac{1}{U_N^2}s^\top\begin{bmatrix}0 & \mathbf{0}\\ \mathbf{0} & I\end{bmatrix}\begin{bmatrix}0 & \mathbf{0}\\ -\mathbf{1} & I\end{bmatrix}X\begin{bmatrix}0 & \mathbf{0}\\ \mathbf{0} & I\end{bmatrix}\bar{s}\\
&\overset{(c)}{=} \frac{1}{U_N^2}s^\top\begin{bmatrix}0 & \mathbf{0}\\ \mathbf{0} & I\end{bmatrix}\begin{bmatrix}0 & \mathbf{0}\\ \mathbf{0} & I\end{bmatrix}X\bar{s}\\
&= \frac{1}{U_N^2}s^\top\begin{bmatrix}0 & \mathbf{0}\\ \mathbf{0} & I\end{bmatrix}\begin{bmatrix}0 & \mathbf{0} & \mathbf{0}\\ \mathbf{0} & M & N\\ \mathbf{0} & N^\top & O\end{bmatrix}\bar{s}\\
&= \frac{1}{U_N^2}s^\top\begin{bmatrix}0 & \mathbf{0} & \mathbf{0}\\ \mathbf{0} & M & N\\ \mathbf{0} & N^\top & O\end{bmatrix}\bar{s}\\
&= \frac{1}{U_N^2}\begin{bmatrix}p^\top + jq^\top\end{bmatrix}X\begin{bmatrix}p - jq\end{bmatrix}\\
&\overset{(d)}{=} \frac{p^\top Xp}{U_N^2} + \frac{q^\top Xq}{U_N^2}
\end{aligned}
\tag{A.2}
$$

where the approximation consists in a term which is $o\left(\frac{1}{U_N^2}\right)$, in (a) we used the fact that Y is symmetric and each row sums to zero, that is $\mathbf{1}^\top Y = Y\mathbf{1} = 0$, equivalence (b) comes from Lemma 1 in Chapter 5 and (c) and (d) are allowed by the symmetry of X.

A.2 Cost function for ADMM approach

Starting from Equation (A.1), it is simple to relate the total line losses to the local power generation (notice that the following equations verify the power conservation, as described in Chapter 7):

$$\begin{aligned}
\bar{u}^\top Y u \cos\theta &= \mathrm{Re}\{(\cos\theta - j\sin\theta)\bar{u}^\top Y u\} \\
&= \mathrm{Re}\{\bar{u}^\top \boldsymbol{Y} u\} \\
&= \mathrm{Re}\left\{ \begin{bmatrix} \bar{u}_1 & \dots & \bar{u}_N \end{bmatrix} \begin{bmatrix} i_1 \\ \vdots \\ i_N \end{bmatrix} \right\} \\
&= \sum_{i\in\mathcal{V}} \mathrm{Re}\{\bar{u}_i i_{\mathrm{Im}}\} \\
&= \sum_{i\in\mathcal{V}} \mathrm{Re}\{u_i \bar{i}_i\} \\
&= \sum_{i\in\mathcal{V}} p_i
\end{aligned}$$

Now, the active power p_i injected by node i can be expressed as:

$$\begin{aligned}
p_i &= \mathrm{Re}\{s_i\} = \mathrm{Re}\{u_i \bar{i}_i\} = \mathrm{Re}\{u_i e^{j\theta} Y^i \bar{u}\} \\
&= \mathrm{Re}\{(\cos\theta + j\sin\theta)(u_{i_{\mathrm{Re}}} + j u_{i_{\mathrm{Im}}}) Y^i (u_{\mathrm{Re}} - j u_{\mathrm{Im}})\} \\
&= \mathrm{Re}\{(\cos\theta + j\sin\theta)(u_{i_{\mathrm{Re}}} Y^i u_{\mathrm{Re}} + u_{i_{\mathrm{Im}}} Y^i u_{\mathrm{Im}} + j(-u_{i_{\mathrm{Re}}} Y^i u_{\mathrm{Im}} + u_{i_{\mathrm{Im}}} Y^i u_{\mathrm{Re}}))\} \\
&= \cos\theta(u_{i_{\mathrm{Re}}} Y^i u_{\mathrm{Re}} + u_{i_{\mathrm{Im}}} Y^i u_{\mathrm{Im}}) + \sin\theta(u_{i_{\mathrm{Re}}} Y^i u_{\mathrm{Im}} - u_{i_{\mathrm{Im}}} Y^i u_{\mathrm{Re}}) \\
&= \begin{bmatrix} \cos\theta u_{i_{\mathrm{Re}}} Y^i - \sin\theta u_{i_{\mathrm{Im}}} Y^i & \cos\theta u_{i_{\mathrm{Im}}} Y^i + \sin\theta u_{i_{\mathrm{Re}}} Y^i \end{bmatrix} \begin{bmatrix} u_{\mathrm{Re}} \\ u_I \end{bmatrix} \\
&= \begin{bmatrix} \cos\theta u_{i_{\mathrm{Re}}} - \sin\theta u_{i_{\mathrm{Im}}} & \cos\theta u_{i_{\mathrm{Im}}} + \sin\theta u_{i_{\mathrm{Re}}} \end{bmatrix} \begin{bmatrix} Y^i & 0 \\ 0 & Y^i \end{bmatrix} \begin{bmatrix} u_{\mathrm{Re}} \\ u_{\mathrm{Im}} \end{bmatrix} \\
&= \begin{bmatrix} u_{i_{\mathrm{Re}}} & u_{i_{\mathrm{Im}}} \end{bmatrix} \begin{bmatrix} \cos\theta & \sin\theta \\ -\sin\theta & \cos\theta \end{bmatrix} \begin{bmatrix} Y^i & 0 \\ 0 & Y^i \end{bmatrix} \begin{bmatrix} u_{\mathrm{Re}} \\ u_{\mathrm{Im}} \end{bmatrix} \\
&= X^\top \begin{bmatrix} \mathbf{1}_{2i-1} & \mathbf{1}_{2i} \end{bmatrix} \begin{bmatrix} \cos\theta & \sin\theta \\ -\sin\theta & \cos\theta \end{bmatrix} \begin{bmatrix} Y^i & 0 \\ 0 & Y^i \end{bmatrix} \begin{bmatrix} I_N \otimes \begin{bmatrix} 1 & 0 \end{bmatrix} \\ I_N \otimes \begin{bmatrix} 0 & 1 \end{bmatrix} \end{bmatrix} X \\
&=: X^\top P_i X
\end{aligned}$$

with

$$X = \begin{bmatrix} u_{1_{\mathrm{Re}}} \\ u_{1_{\mathrm{Im}}} \\ u_{2_{\mathrm{Re}}} \\ u_{2_{\mathrm{Im}}} \\ \vdots \end{bmatrix} \in \mathbb{R}^{2N}$$

Furthermore, we can underline the local dependence of p_i only on the voltages of node i itself and all nodes j which are neighbours of i: this is due to the fact that the j-th element of the i-th row Y^i of Y is non-zero if and only if $j \in \mathcal{N}(i) \cup \{i\}$; we have:

$$\begin{aligned}
p_i &= \mathrm{Re}\{s_i\} = \mathrm{Re}\{u_i \bar{i}_i\} = \mathrm{Re}\{u_i e^{j\theta} Y^i \bar{u}\} \\
&= \mathrm{Re}\{u_i e^{j\theta} Y^i_{\mathrm{loc}} \bar{u}^i\} \\
&= \begin{bmatrix} u_{i_{\mathrm{Re}}} & u_{i_{\mathrm{Im}}} \end{bmatrix} \begin{bmatrix} \cos\theta & \sin\theta \\ -\sin\theta & \cos\theta \end{bmatrix} \begin{bmatrix} Y^i_{\mathrm{loc}} & 0 \\ 0 & Y^i_{\mathrm{loc}} \end{bmatrix} \begin{bmatrix} u^i_{\mathrm{Re}} \\ u^i_{\mathrm{Im}} \end{bmatrix} \\
&= X^{i\top} \begin{bmatrix} I_2 \\ 0_{2|\mathcal{N}(i)|\times 2} \end{bmatrix} \begin{bmatrix} \cos\theta & \sin\theta \\ -\sin\theta & \cos\theta \end{bmatrix} \begin{bmatrix} Y^i_{\mathrm{loc}} & 0 \\ 0 & Y^i_{\mathrm{loc}} \end{bmatrix} \begin{bmatrix} I_{|\mathcal{N}(i)|+1} \otimes \begin{bmatrix} 1 & 0 \end{bmatrix} \\ I_{|\mathcal{N}(i)|+1} \otimes \begin{bmatrix} 0 & 1 \end{bmatrix} \end{bmatrix} X^i
\end{aligned}$$

where

$$u^i = \begin{bmatrix} u_i \\ u_{j_1} \\ u_{j_2} \\ \vdots \end{bmatrix} \in \mathbb{C}^{|\mathcal{N}(i)|+1}, \; X^i = \begin{bmatrix} u_{i_{\mathrm{Re}}} \\ u_{i_{\mathrm{Im}}} \\ u_{j_{1_{\mathrm{Re}}}} \\ u_{j_{1_{\mathrm{Im}}}} \\ \vdots \end{bmatrix} \in \mathbb{R}^{2|\mathcal{N}(i)|+2}$$

$$Y^i_{\mathrm{loc}} = \begin{bmatrix} Y_{i,i} & Y_{i,j_1} & Y_{i,j_2} & \dots \end{bmatrix}$$

B

ADMM Lagrangian derivation

In this appendix the calculations that allow to obtain Equation (7.15) are shown.

$$
\begin{aligned}
&\mathcal{L}^i(X^{(i)}, Z^{(i)}(t), \Lambda^{(i)}(t)) = \\
&= p_i(X^{(i)}) + \sum_{j\in\mathcal{N}(i)} \Big[2\lambda_i^{(i,j)}(t)x_i^{(i)} + 2\lambda_j^{(i,j)}(t)x_j^{(i)}\Big] \\
&\qquad + \rho \sum_{j\in\mathcal{N}(i)} \Big[\|x_i^{(i)}\|^2 - 2x^{(i)^\top} z_i^{(i,j)}(t) + \|x_j^{(i)}\|^2 - 2x_j^{(i)^\top} z_j^{(i,j)}(t)\ \Big]\Big\} \\
&= p_i(X^{(i)}) + 2\left[\textstyle\sum_{j\in\mathcal{N}(i)} \lambda_i^{(i,j)} \quad \{\lambda_j^{(i,j)}\}_{j\in\mathcal{N}(i)}\right] \begin{bmatrix} x_i^{(i)} \\ \{x_j^{(i)}\}_{j\in\mathcal{N}(i)} \end{bmatrix} \\
&\qquad + \rho|\mathcal{N}(i)|x_i^{(i)\top}x_i^{(i)} - 2\rho x_i^{(i)\top} \sum_{j\in\mathcal{N}(i)} z_i^{(i,j)}(t) \\
&\qquad + \rho \sum_{j\in\mathcal{N}(i)} x_j^{(i)\top}x_j^{(i)} - 2\rho \sum_{j\in\mathcal{N}(i)} x_j^{(i)\top} z_j^{(i,j)}(t) \\
&= p_i(X^{(i)}) + 2F^{(i)}(t)X^{(i)} + \rho\big(|\mathcal{N}(i)|x_i^{(i)\top}x_i^{(i)} + \sum_{j\in\mathcal{N}(i)} x_j^{(i)\top}x_j^{(i)}\big) \\
&\qquad - 2\rho\Big(x_i^{(i)\top} \sum_{j\in\mathcal{N}(i)} \frac{x_i^{(i)}(t) + x_i^{(j)}(t)}{2} + \sum_{j\in\mathcal{N}(i)} x_j^{(i)\top} \frac{x_j^{(i)}(t) + x_j^{(j)}(t)}{2}\Big) \\
&= p_i(X^{(i)}) + 2X^{(i)\top}F^{(i)}(t)^\top + \rho\left[x_i^{(i)\top} \quad \{x_j^{(i)\top}\}_{j\in\mathcal{N}(i)}\right] \begin{bmatrix} |\mathcal{N}(i)|I_2 & 0 \\ 0 & I \end{bmatrix} \begin{bmatrix} x_i^{(i)} \\ \{x_j^{(i)}\}_{j\in\mathcal{N}(i)} \end{bmatrix}
\end{aligned}
$$

$$
\begin{aligned}
&\quad - \rho \begin{bmatrix} x_i^{(i)\top} & \{x_j^{(i)\top}\}_{j\in\mathcal{N}(i)} \end{bmatrix} \begin{bmatrix} \sum_{j\in\mathcal{N}(i)} x_i^{(i)}(t) + x_i^{(j)}(t) \\ \{x_j^{(i)}(t) + x_j^{(j)}(t)\}_{j\in\mathcal{N}(i)} \end{bmatrix} \\
&= p_i(X^{(i)}) + \rho X^{(i)\top} \begin{bmatrix} |\mathcal{N}(i)| I_2 & 0 \\ 0 & I \end{bmatrix} X^{(i)} \\
&\quad + X^{(i)\top} \Bigg(2F^{(i)\top}(t) - \rho \begin{bmatrix} |\mathcal{N}(i)| I_2 & 0 \\ 0 & I \end{bmatrix} X^{(i)}(t) - \rho \begin{bmatrix} \sum_{j\in\mathcal{N}(i)} x_i^{(j)}(t) \\ \{x_j^{(j)}(t)\}_{j\in\mathcal{N}(i)} \end{bmatrix} \Bigg) \\
&= p_i(X^{(i)}) + \rho X^{(i)\top} \begin{bmatrix} |\mathcal{N}(i)| I_2 & 0 \\ 0 & I \end{bmatrix} X^{(i)} - X^{(i)\top} \Bigg(-2F^{(i)\top}(t) \\
&\quad - \rho \begin{bmatrix} |\mathcal{N}(i)| I_2 & 0 \\ 0 & I \end{bmatrix} X^{(i)}(t) + 2\rho \begin{bmatrix} |\mathcal{N}(i)| I_2 & 0 \\ 0 & I \end{bmatrix} X^{(i)}(t) + \rho \begin{bmatrix} \sum_{j\in\mathcal{N}(i)} x_i^{(j)}(t) \\ \{x_j^{(j)}(t)\}_{j\in\mathcal{N}(i)} \end{bmatrix} \Bigg) \\
&= p_i(X^{(i)}) + X^{(i)\top} M_i X^{(i)} - X^{(i)\top} \big(2M_i X^{(i)}(t) + G^{(i)}(t) - 2F^{(i)\top}(t) \big) \\
&= p_i(X^{(i)}) + X^{(i)\top} M_i X^{(i)} - X^{(i)\top} B^{(i)}(t)
\end{aligned}
$$

Bibliography

[1] Directorate-General for Research Sustainable Energy Systems, "European Technology Platform SmartGrids - Vision and Strategy for Europe's Electricity Networks of the Future", 2006. Available: ftp://ftp.cordis.europa.eu/pub/fp7/energy/docs/smartgrids_en.pdf

[2] http://www.enel.it/it-IT/reti/enel_distribuzione/qualita/progetti_smart_grids/

[3] S. Bolognani and S. Zampieri, "A distributed control strategy for reactive power compensation in smart microgrids", *arXiv*, arXiv:1106.5626v3 [math.OC], October 2012. Available: http://arxiv.org/pdf/1106.5626.pdf

[4] G. Cavraro, "Algoritmi per la Compensazione Distribuita della Potenza Reattiva nelle Smart Grid", Master's thesis, Mar. 2011.

[5] A. Biral, "Ottimizzazione nelle Smart Grid: Soluzione Centralizzata e Distribuita", Master's thesis, Dec. 2013.

[6] A.Y.S. Lam, B. Zhang and A. Dominguez-Garcia, D. Tse, "Optimal Distributed Voltage Regulation in Power Distribution Networks", pp. 1-2, April 2012.

[7] M. Guarnieri, "Elementi di elettrotecnica circuitale", Edizioni Progetto - Padova, pp. 279-460, 2010.

[8] G. Andersson, "Modelling and Analysis of Electric Power Systems", EEH - Power Systems Laboratory, ETH Zürich, September 2008.

[9] R. D. Zimmerman, C. E. Murillo-Sánchez, and R. J. Thomas, "MATPOWER: Steady-State Operations, Planning and Analysis Tools for Power Systems Research and Education", *Power Systems, IEEE Transactions on*, vol. 26, no. 1, pp. 12-19, Feb. 2011. See also: `http://www.pserc.cornell.ed/matpower/`

[10] W. H. Kersting, "Radial distribution test feeders," *Transaction on Power Systems*, vol. 6, no. 3, pp. 975–985, August 1991.

[11] S. Bolognani, R. Carli, G. Cavraro, and S. Zampieri, "A distributed feedback control strategy for optimal reactive power flow with voltage constraints", 2012, arXiv preprint available [math.OC] 1303.7173.

[12] S. Bolognani, R. Carli, G. Cavraro, S. Zampieri, "A distributed control strategy for optimal reactive power flow with power constraints", *52st IEEE Conference on Decision and Control (CDC 2013)*, Florence, Italy, 2013.

[13] S. Bolognani, R. Carli, G. Cavraro, S. Zampieri, "A distributed control strategy for optimal reactive power flow with power and voltage constraints", *SmartGridComm 2013*, Vancouver, Canada, 2013.

[14] J. Lavaei and S. H. Low, "Zero duality gap in optimal power flow problem", *IEEE Trans. Power Syst.*, 2011.

[15] S. Boyd and L. Vandenberghe, *Convex Optimization*, Cambridge, U.K.: Cambridge University Press, 2004.

[16] Tomaso Erseghe, "A distributed and scalable processing method based upon ADMM", *IEEE Signal Processing Letters*, vol. 19, no. 9, pp.563-566, September 2012.

[17] D. P. Bertsekas and J. N. Tsitsiklis, *Parallel and distributed computation: numerical methods*, Thena Scientific, 1997.

[18] B. Zhao, C. X. Guo, and Y. J. Cao, "A multiagent-based particle swarm optimization approach for optimal reactive power dispatch", *IEEE Trans. Power Syst.*, vol. 20, no. 2, pp. 1070-1078, May 2005.

[19] F. Katiraei and M. R. Iravani, "Power management strategies for a microgrid with multiple distributed generation units", *IEEE Trans. Power Syst.*, vol. 21, no. 4, pp. 1821-1831, Nov. 2006.

[20] S. Boyd, N. Parikh, E. Chu, B. Peleato, and J. Eckstein, "Distributed optimization and statistical learning via the alternating direction method of multipliers". *Foundations and Trends in Machine Learning*, vol. 3, no. 1, pp. 1-122, 2011.

[21] J. Lavaei, D.Tse, and B. Zhang, "Geometry of power flows in tree networks", in *To appear in Proc. of PES 2012 General Meetings*, 2012.

[22] B.C. Lesieutre, D.K. Molzahn, A.R. Borden, and C.L. DeMarco, "Examining the Limits of the Application of Semidefinite Programming to Power Flow Problems", *49th Annual Allerton Conference on Communication, Control, and Computing (Allerton), 2011*, pp.1492-1499, 28-30 Sept. 2011.

[23] A. Costabeber, T. Erseghe, P. Tenti, S. Tomasin, and P. Mattavelli, "Optimization of micro-grid operation by dynamic grid mapping and token ring control", in *Proc. 14th European Conf. on Power Electronics and Applications (EPE)*, Birmingham, UK, 2011.

[24] E. Dall'Anese, H. Zhu, G. B. Giannakis, "Distributed Optimal Power Flow for Smart Microgrids", *IEEE Trans. Smart Grid 4*, no. 3, pp. 1464-1475, 2013.

[25] M. Prodanovic, K. De Brabandere, J. Van den Keybus, T. Green, and J. Driesen, "Harmonic and reactive power compensation as ancillary services in inverter-based distributed generation", *IET Gener. Transm. Distrib.*, vol. 1, no. 3, pp. 432-438, 2007.

[26] A. Ghosh, S. Boyd, and A. Saberi, "Minimizing effective resistance of a graph", *SIAM Rev.*, vol. 50, no. 1, pp. 37-66, Feb. 2008.

[27] S. Bolognani, N. Bof, D. Michelotti, R. Muraro, L. Schenato, "Identification of power distribution network topology via voltage correlation analysis", *Conference on Decision and Control (CDC13)*, 2013.

Ecco che in questa pagina si conclude la mia tesi magistrale e, con essa, una vera e propria epoca della mia vita. Ritengo sia giunta l'ora di tirare un po' le somme di quanto accaduto in questi mesi e anni, dedicando qualche riga a quanti mi hanno regalato momenti, anche brevi, di felicità.

Desidero innanzitutto esprimere i miei più vivi ringraziamenti al mio relatore, il Prof. Ruggero Carli, e al dottorando che mi ha aiutato, Guido Cavraro, perchè hanno saputo indirizzarmi nel lavoro offrendomi, da una parte, importanti delucidazioni e, dall'altra, un clima di lavoro che mi ha fatto rendere al meglio delle mie possibilità.

Passando poi al lato più personale, voglio ovviamente ringraziare i miei genitori e mio fratello, sempre presenti con il loro affetto e una buona dose di saggi consigli: dedico a voi questo lavoro e, di riflesso, tutto ciò che ho fatto in questi anni di formazione scolastica/universitaria.

A ruota voglio ringraziare quella che ormai è a tutti gli effetti la nuova componente della famiglia, Federica, di cui sono sempre più innamorato: se prima ho dedicato ciò che è stato, spero di dedicare a te ciò che sarà. Con lei ringrazio Mauro e Luisa, sempre così affettuosi nei miei confronti.

Un grazie a nonna Adriana (dai che hai visto anche questa!), ai nonni che rimangono vivi nei miei ricordi, agli zii e ai cugini tutti, che sempre dimostrano di essere fieri di me.

Grazie ai miei amici dell'asse Torreglia-Guizza (Zec, Monti, Ale, Pippo, Diego, Marti, Marco, Eli, Bongo, and so on!) che con semplicemente il loro modo di essere mi hanno fatto conoscere ed apprezzare le cose più significative della vita, rendendola inoltre più divertente!

Grazie ai miei compagni di scuola e corso, che hanno reso indimenticabili questi quadrimestri/semestri tra i banchi: per questi ultimi due anni voglio citare almeno Matteo, Martina, Luca e Nicoletta, ma ce ne sarebbero altri!

Grazie alla mia squadra di calcetto e a tutte quelle precedenti di calcio, che mi da e mi hanno dato l'opportunità di praticare l'arte dello sbaeonare!

In the end, thanks to Helsinki, where I spent one of the happiest periods of my life. That was possible thanks to the presence of Eddy, Viola, Fabrizio, Andrea, Eva, Paty, Miryam, Juan Carlos, Daniel, Quentin and many others!

Grazie a tutti!